# Pyrimidine and Purine Mononucleotides Recognition by Trivalent Lanthanide Complexes with *N*-Acetyl Amino Acids

**Hassan A. Azab,* Zeinab M. Anwar, and Rasha G. Ahmed**

Chemistry Department, Faculty of Science, Suez Canal University, Ismailia 41522, Egypt

Potentiometric equilibrium measurements have been performed at (25.0 ± 0.1) °C and ionic strength $I$ = 0.1 mol·dm$^{-3}$ $KNO_3$ for the interaction of the biologically important ligands *N*-acetylhistidine, *N*-acetyl L-leucine, *N*-acetylglutamic acid, *N*-acetylhistamine, *N*-acetylaspartic acid, and La(III), Gd(III), Sm(III), Tb(III), Eu(III), and Dy(III) with the nucleotides guanosine 5′-monophosphate (5′-GMP), cytedine 5′-monophosphate (5′-CMP), inosine 5′-monophosphate (5′-IMP), adenosine 5′-monophosphate (5′-AMP), adenosine 5′-diphosphate (5′-ADP), adenosine 5′-triphosphate (5′-ATP), and cytedine 5′-triphosphate (5′-CTP) in 1:1:1 and 1:2:1 ratios. The formation constants of various mixed ligand complexes were inferred from the potentiometric titration curves. Initial estimates of the formation constants of the resulting species and the formation constants of the different *N*-acetyl amino acid (NAA) and nucleotide (NU) complexes in metal ligand ratios 1:1 and 2:1 have been refined with the SUPERQUAD computer program. Confirmation of the formation of binary and ternary complexes of the type Ln(III)−NU−NAA and the possible recognition of the purine and pyrimidine mononucleotides by *N*-acetyl amino acid complexes of lanthanides in aqueous media have been carried out using UV spectroscopic and fluorimetric measurements.

## Introduction

Lanthanide ions have interested bioinorganic chemists for decades because of their versatility in probing calcium functional sites in vivo, as well as their application and promise as pharmaceutical agents. These ions have unique spectroscopic properties such as sharp luminescence emission and strong paramagnetic shift properties and display a preference for coordination environments that parallel that of $Ca^{2+}$ ions. Thus, lanthanide ion complexes with various versatile ligands is a promising field. The four lanthanide ions Tb(III), Eu(III), Sm(III), and Dy(III) exhibit characteristic emission spectra with narrow line-shaped emission bands in the visible range of the electromagnetic spectrum. However, it is hard to evoke the emission because of the low molar absorptivity of the naked metal ions. This problem can be solved through the complexation of lanthanide ions to organic ligands possessing energy levels close to those of the metal ions. It is possible to excite the ligand by irradiation of light at its characteristic excitation wavelength. The absorbed energy is then transferred from the ligand to the central lanthanide ion, which subsequently emits light at its characteristic wavelengths. Lanthanide luminescence has evolved to become a highly sensitive and selective detection method. Lanthanide chelates have become popular labels for immunoassays.[1]

*N*-Acetyl amino acids are versatile promising ligands since they possess important biological importance. *N*-Acetyl-L-aspartic acid (NAAsp) is an unusual amino acid that is present in the brain of vertebrates.[2] Its concentration is one of highest of all amino acids, and although NAAsp is synthesized and stored primarily in neurons, it can not be hydrolyzed in these cells. Furthermore, neuronal NAAsp is dynamic and turns over more than once, each day by cycling via extracellular fluids (ECF), between neurons and catabolic compartments in oligodendrocytes. While NAAsp may have several functions in the central nervous system (CNS), an important role of the NAAsp system appears to be osmoregulatory, and in this role it may be the primary mechanism for the removal of metabolic water.[3] It has also been proposed that NAAsp may operate as a molecular water pump (MWP) in neurons[4,5] with NAAsp diffusing down its gradient into extracellular fluids (ECF) as NAAsp-obligated water is transported out of neurons against a water gradient.

The α-*N*-acetyl-α-amino acid methylamides derived from glycine, L-alanine, L-isoleucine, L-methionine, L-proline, L-hydroxyproline, L-histidine, D- and L-phenylalanine, D- and L-tyrosine, and D- and L-tryptophan have been examined with respect to their ability to inhibit the α-chymotrypsin catalyzed hydrolysis of benzoyl-L-valine methyl ester. The extent of interaction of the enzyme with the first seven compounds was insufficient to permit evaluation of the enzyme-inhibitor dissociation constants, beyond assignment of a lower limit for the magnitude of these constants.[6]

*N*-Acetyl-aspartate is an abundant [(5 to 10) mM] amino acid derivative of the nervous system[7] and is used clinically as a noninvasive marker for the functional integrity of neurons using magnetic resonance spectroscopy.[8,9] Aspartate-*N*-acetyltransferase (ASP-NAT; EC2.3.1.17) catalyzes acetylation of L-aspartate (Asp) by acetyl CoA to form NAAsp.[10−12] Earlier studies have shown that NAAsp is localized primarily in neurons[13−15] and also demonstrated in cultured oligodendrocytes.[16]

The importance of NAAsp in neuronal functions has been further emphasized by recent reports that show a strong association between NAAsp and cognitive ability and intelligence in humans.[17,18] Also, decreased degradation of NAAsp resulting from a congenital defect in the degradative enzyme aspartocylase (EC3.5.1.15) causes Canavan's disease, an auto-

* Corresponding author. E-mail: hazab@daad-alumni.de.

10.1021/je9004118 CCC: $40.75 
Published on Web 10/02/2009

somal recessive neurodegenerative disorder that develops after birth and results in death before 10 years of age.[19]

*N*-Acetyl-aspartate is the major intracellular brain metabolite detectable using $^1$H MRS. NAAsp production and mitochondrial metabolism are inextricably linked, as NAAsp is synthesized solely in brain mitochondria.[20] Decreases in the activity of mitochondrial respiratory chain enzyme activities have been shown to result in a decreased capacity of brain mitochondria to synthesize NAAsp.[21]

*N*-Acetyl-L-aspartate is the second most abundant free amino acid in the mammalian brain next to glutamate.[22−24] NAAsp is located primarily in neurons at concentrations of approximately 10 mM.[25−29] Perturbations in NAAsp levels in the brain due to various pathological conditions have been detected with proton NMR spectroscopy. An elevation in NAAsp concentrations has been measured in Canavan's disease due to a lack of aspartoacylase (acylase II), the enzyme responsible for the break down of NAAsp.[30] Decreases in NAAsp concentrations have been found in Huntington's disease,[31] amyotrophic lateral sclerosis,[32] Alzheimer's disease,[33] traumatic brain injury,[29] ischemic injuries,[34] multiple sclerosis,[35] HIV,[36] and schizophrenia.[37] In the brain, NAAsp is synthesized and stored in the neurons but is hydrolyzed in glial cells.[30]

NAAsp and *N*-acetyl-aspartate-L-glutamate ligase (NAAG) are major neuronal osmolytes, and in this capacity they can also serve as a cellular reservoir for Asp and Glu. In addition, as they are polar and ionizable hydrophilic molecules that undergo a regulated efflux into ECF, both probably play a role in water movement out of neurons.[38] NAAsp appears not to exhibit any neurotransmitter activity.[39] However, NAAG does, and thus it may have additional roles as a neurotransmitter in the CNS, acting as a partial agonist of *N*-methyl-D-aspartate receptors, and in a selective activation of the metabotropic Glu receptor $mGluR_3$ in astrocytes,[40,41] although NAAsp has been shown to be important osmotically and for myelin synthesis.

The formation constants for the binary and ternary complexes containing La(III), Ce(III), Pr(III), or Eu(III) and 5′-GMP, 5′-AMP, and 5′-CMP with zwitterionic buffers (MOPSO, MES, ACES, or HEPES) were determined at $I = 0.1$ mol·dm$^{-3}$ $KNO_3$ and at 25.0 °C. The values were obtained for the different complex species through potentiometric measurements.[42]

In this work, we report the formation constant values for the interaction of the studied lanthanides [La(III), Gd(III), Sm(III), Tb(III), Eu(III), or Dy(III)] with two categories of biologically important ligands, *N*-acetylamino acids (*N*-acetyl histidine, *N*-acetyl L-leucine, *N*-acetylglutamic acid, *N*-acetylhistamine, and *N*-acetylaspartic acid) and nucleotides (5′-GMP, 5′-CMP, 5′-IMP, 5′-AMP, 5′-ATP, and 5′-CTP), in their binary form as mono- and dinuclear complexes and the corresponding mixed ligand complexes (1:1:1). Also, the absorption and emission spectra of the different species formed are examined.

## Experimental Section

***Materials and Solutions.*** All materials employed in the present investigation were A.R. grade products. Guanosine 5′-monophosphate (5′-GMP), inosine 5′-monophosphate (5′-IMP), adenosine 5′-monophosphate (5′-AMP), cytidine 5′-monophosphate (5′-CMP), adenosine 5′-triphosphate (5′-ATP), cytidine 5′-triphosphate (5′-CTP), and adenosine 5′-diphosphate (5′-ADP) were purchased from the Sigma Chemical Co. and were used without purification. Reagent grade *N*-acetylhistamine, *N*-acetylhistidine, *N*-acetylaspartic acid, *N*-acetylglutamic acid, *N*-acetylleucine, and *N*-acetyllysine were obtained from the Sigma Chemical Co., St. Louis, MO. The purity for these compounds averaged 99.5 %. A $CO_2$-free solution of potassium hydroxide (Merck AG) was prepared and standardized against multiple samples of primary-standard potassium hydrogen phthalate (Merck AG) under $CO_2$-free conditions. $KNO_3$, KOH, and nitric acid were from Merck AG Darmstadt, Germany. Lanthanide metal salts $La(NO_3)_3 \cdot 5H_2O$, $Gd(NO_3)_3 \cdot 6H_2O$, $Sm(NO_3)_3 \cdot 6H_2O$, $Tb(NO_3)_3 \cdot 6H_2O$, $Eu(NO_3)_3 \cdot 6H_2O$, and $Dy(NO_3)_3 \cdot 6H_2O$ were from the Sigma Chemical Co.

***Apparatus and Procedures.*** Potentiometric pH measurements were made on solutions in a double-walled glass vessel at [(25.0 ± 0.1) °C] with commercial Fisher combined electrode, and a magnetic stirrer was used. A Fisher account pH/ion meter model/825 MP was used. Purified nitrogen was bubbled through the solutions during titrations, and the titrant KOH solution was added by an automatic dispenser. The test solutions were titrated with standard $CO_2$-free KOH.

The electrodes were calibrated in both the acidic and alkaline regions by titrating 0.01 mol·dm$^{-3}$ nitric acid with standard potassium hydroxide under the same experimental conditions. The concentration of free hydrogen ion, $C_H^+$, at each point of the titration is related to the measured, $E$, of the cell by the Nernst equation.

$$E = E^\circ + Q \log C_H^+ \quad (1)$$

where $E^\circ$ is a constant that includes the standard potential of the glass electrode and $Q$ is the slope of the glass electrode response. The value of $E^\circ$ for the electrode was determined from a Gran plot derived from a separate titration of nitric acid with standard KOH under the same temperature and medium conditions as for the test solution titration.

The results so obtained were analyzed by the nonlinear least-squares computer program ESAB2M[43] to refine $E^\circ$ and the autoprotolysis constant of water, $K_w$.

During these calculations, the $K_w$ was refined until the best value for $Q$ was obtained. The results obtained indicated the reversible Nernstain response of the glass electrode used.

The solutions titrated can be presented according to the following scheme:

(a) $2 \cdot 10^{-3}$ mol·dm$^{-3}$ $HNO_3$ + $5 \cdot 10^{-4}$ mol·dm$^{-3}$ *N*-acetylamino acids

(b) $2 \cdot 10^{-3}$ mol·dm$^{-3}$ $HNO_3$ + $5 \cdot 10^{-4}$ mol·dm$^{-3}$ *N*-acetylamino acids + $5 \cdot 10^{-4}$ mol·dm$^{-3}$ M(III) (binary complex)

(c) $2 \cdot 10^{-3}$ mol·dm$^{-3}$ $HNO_3$ + $5 \cdot 10^{-4}$ mol·dm$^{-3}$ nucleotides (GMP, CMP, IMP, AMP, CTP, ADP, and ATP)

(d) $2 \cdot 10^{-3}$ mol·dm$^{-3}$ $HNO_3$ + $5 \cdot 10^{-4}$ mol·dm$^{-3}$ nucleotides + $5 \cdot 10^{-4}$ mol·dm$^{-3}$ M(III) (binary complexes)

(e) $2 \cdot 10^{-3}$ mol·dm$^{-3}$ $HNO_3$ + $5 \cdot 10^{-4}$ mol·dm$^{-3}$ *N*-acetylamino acids + $5 \cdot 10^{-4}$ mol·dm$^{-3}$ nucleotides + $5 \cdot 10^{-4}$ mol·dm$^{-3}$ M(III) (ternary complexes)

(f) $2 \cdot 10^{-3}$ mol·dm$^{-3}$ $HNO_3$ + $5 \cdot 10^{-4}$ mol·dm$^{-3}$ nucleotides + $1 \cdot 10^{-3}$ mol·dm$^{-3}$ M(III) (dinuclear complex)

(g) $2 \cdot 10^{-3}$ mol·dm$^{-3}$ $HNO_3$ + $5 \cdot 10^{-3}$ mol·dm$^{-3}$ *N*-acetylamino acids + $1 \cdot 10^{-3}$ mol·dm$^{-3}$ M(III) (dinuclear complex)

where M(III) = Sm(III), La(III), Gd(III), Eu(III), Dy(III), and Tb(III); nucleotides = GMP, CMP, IMP, AMP, CTP, ADP, and ATP, *N*-acetylamino acids = *N*-acetylhistamine, *N*-acetylhistidine, *N*-acetylaspartic acid, *N*-acetylglutamic acid, *N*-acetylleucine, and *N*-acetyllysine.

A constant ionic strength was maintained by adding 0.1 mol·dm$^{-3}$ $KNO_3$, and the total volume was kept constant at 10 cm$^3$. At least four titrations were performed for each system. For both ligand protonation and metal complex formation equilibria, data were collected over the largest possible pH interval, although a number of expermintal points were fre-

**Scheme 1. Structures of the Studied Ligands**

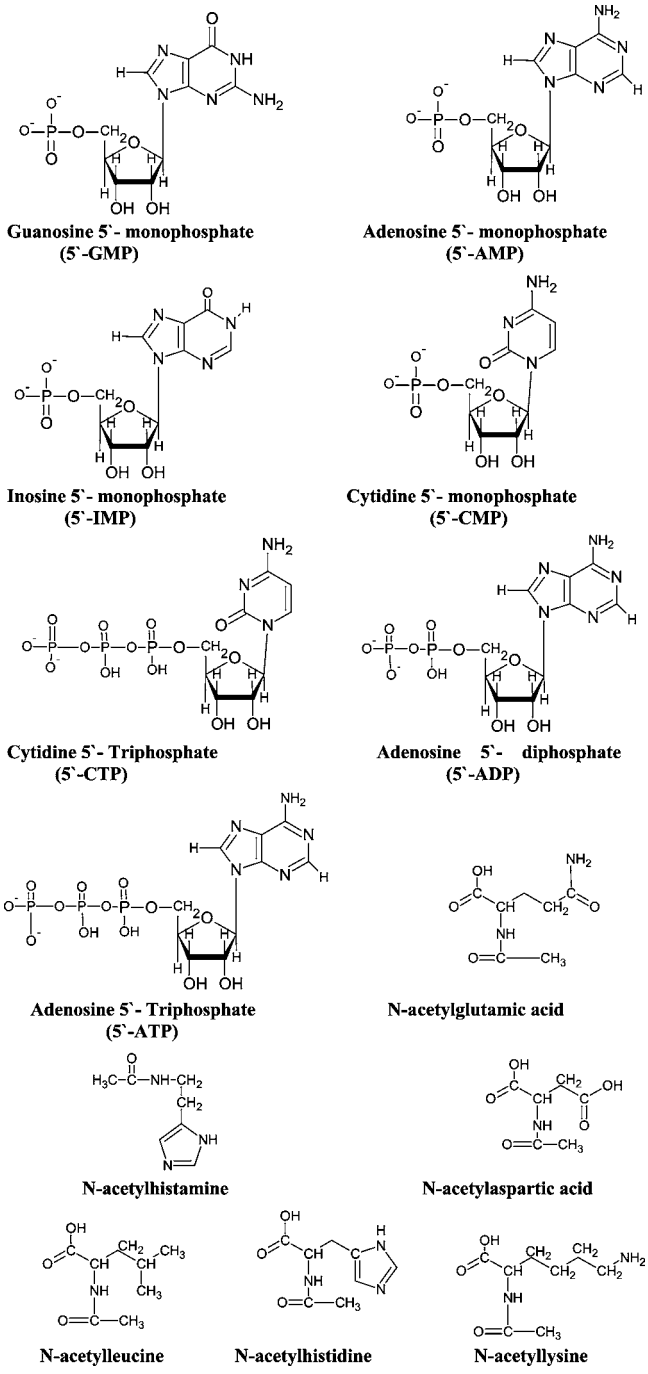


quently discarded for the final stability constant calculations, especially within the range where the complexation observed was insignificant. Initial estimates of the formation constants of ternary complexes in a 1:1:1 ratio and the stability constants of the binary 1:1 and 2:1 complexes have been refined using the SUPERQUAD computer program.[44]

The formation of the ternary complex species occurs via two different mechanisms. The first one is the stepwise mechanism, where it follows two steps (charges are omitted for clarity)

$$pM + q(NU) + sH \rightleftharpoons (M)p(NU)q(H)s \qquad (2)$$

i.e., the lanthanide metal ion reacts with the primary ligand (nucleotide). Hence, the second step is the reaction of the formed binary complex with the *N*-acetylamino acid as the secondary ligand.

**Table 1. Formation Constants of Ln(III)−Nucleotide Binary Complexes in 1:1 and 2:1 Ratio[a,b]**

| lanthanide metal ion | GMP | | IMP | | AMP | | ADP | | ATP | | CMP | | CTP | |
|---|---|---|---|---|---|---|---|---|---|---|---|---|---|---|
| Ln(III) | log $K_{M(NU)}$ | log $K_{M2(NU)}$ | log $K_{M(NU}$ | log $K_{M2(NU)}$ | log $K_{M(NU)}$ | log $K_{M2(NU)}$ | log $K_{M(NU)}$ | log $K_{M2(NU)}$ | log $K_{M(NU)}$ | log $K_{M2(NU)}$ | log $K_{M(NU)}$ | log $K_{M2(NU)}$ | log $K_{M(NU)}$ | log $K_{M2(NU)}$ |
| La(III) | 3.57 ± 0.02 | 7.20 ± 0.03 | 5.05 ± 0.02 | 7.12 ± 0.03 | 3.87 ± 0.02 | 7.04 ± 0.02 | 3.53 ± 0.02 | 6.72 ± 0.03 | 3.69 ± 0.02 | 7.24 ± 0.03 | 3.13 ± 0.02 | 7.18 ± 0.03 | 3.60 ± 0.03 | 7.18 ± 0.04 |
| Sm(III) | 6.71 ± 0.02 | 7.20 ± 0.03 | 6.08 ± 0.03 | 9.40 ± 0.02 | 4.97 ± 0.02 | 9.48 ± 0.02 | 3.22 ± 0.02 | 7.20 ± 0.03 | 3.62 ± 0.02 | 7.20 ± 0.02 | 3.60 ± 0.02 | 7.20 ± 0.02 | 3.15 ± 0.02 | 7.20 ± 0.03 |
| Eu(III) | 4.04 ± 0.02 | 7.18 ± 0.03 | 5.65 ± 0.02 | 7.24 ± 0.03 | 3.64 ± 0.02 | 7.20 ± 0.03 | 4.8 ± 0.02 | 3.6 ± 0.02 | 3.76 ± 0.02 | 7.20 ± 0.03 | 3.67 ± 0.02 | 7.18 ± 0.02 | 3.58 ± 0.02 | 7.6 ± 0.03 |
| Gd(III) | 5.04 ± 0.02 | 7.22 ± 0.03 | 3.90 ± 0.02 | 7.20 ± 0.02 | 4.19 ± 0.02 | 7.6 ± 0.03 | 3.86 ± 0.01 | 7.20 ± 0.02 | 3.61 ± 0.01 | 7.50 ± 0.02 | 4.15 ± 0.01 | 7.22 ± 0.02 | 3.34 ± 0.01 | 7.20 ± 0.02 |
| Tb(III) | 4.21 ± 0.02 | 7.20 ± 0.02 | 4.00 ± 0.01 | 7.20 ± 0.02 | 3.61 ± 0.01 | 7.20 ± 0.02 | 3.58 ± 0.02 | 7.20 ± 0.02 | 3.60 ± 0.02 | 7.24 ± 0.02 | 3.38 ± 0.01 | 7.20 ± 0.02 | 3.64 ± 0.01 | 9.54 ± 0.02 |
| Dy(III) | 6.54 ± 0.02 | 7.64 ± 0.02 | 4.33 ± 0.01 | 7.20 ± 0.02 | 3.80 ± 0.01 | 7.20 ± 0.02 | 3.59 ± 0.01 | 7.24 ± 0.02 | 3.53 ± 0.01 | 7.50 ± 0.02 | 3.14 ± 0.01 | 9.07 ± 0.03 | 3.39 ± 0.01 | 7.20 ± 0.03 |

[a] $I = 0.1$ mol·dm$^{-3}$ $KNO_3$ and at 25 °C. [b] ± Refers to three times standard deviation.

**Table 2. Formation Constants of Ln(III)−*N*-Acetylamino Acid Binary Complexes in 1:1 and 2:1 Ratio**[a,b]

| lanthanide metal ion | *N*-acetylaspartic acid | | *N*-acetylglutamic acid | | *N*-acetylhistidine | | *N*-acetylhistamine | | *N*-acetylleucine | | *N*-acetyllysine | |
|---|---|---|---|---|---|---|---|---|---|---|---|---|
| Ln(III) | log $K_{M(NAA)}$ | log $K_{M2(NAA)}$ | log $K_{M(NAA)}$ | log $K_{M2(NAA)}$ | log $K_{M(NAA)}$ | log $K_{M2(NAA)}$ | log $K_{M(NAA)}$ | log $K_{M2(NAA)}$ | log $K_{M(NAA)}$ | log $K_{M2(NAA)}$ | log $K_{M(NAA)}$ | log $K_{M2(NAA)}$ |
| La(III) | 3.48 ± 0.01 | 9.22 ± 0.03 | 3.58 ± 0.01 | 6.96 ± 0.02 | 4.75 ± 0.02 | 6.92 ± 0.02 | 3.68 ± 0.02 | 6.64 ± 0.02 | 4.68 ± 0.02 | 6.64 ± 0.02 | 5.02 ± 0.02 | 6.90 ± 0.03 |
| Sm(III) | 3.60 ± 0.01 | 7.18 ± 0.02 | 3.59 ± 0.01 | 7.18 ± 0.03 | 5.69 ± 0.02 | 7.18 ± 0.03 | 3.69 ± 0.02 | 7.18 ± 0.02 | 4.10 ± 0.01 | 7.18 ± 0.02 | 6.58 ± 0.02 | 7.18 ± 0.03 |
| Eu(III) | 3.59 ± 0.01 | 7.18 ± 0.02 | 3.61 ± 0.01 | 7.16 ± 0.03 | 5.20 ± 0.02 | 7.20 ± 0.03 | 3.67 ± 0.02 | 7.22 ± 0.02 | 9.33 ± 0.02 | 7.39 ± 0.02 | 6.22 ± 0.02 | 9.32 ± 0.03 |
| Gd(III) | 3.61 ± 0.02 | 7.18 ± 0.02 | 3.59 ± 0.01 | 7.18 ± 0.02 | 5.01 ± 0.02 | 7.19 ± 0.03 | 3.60 ± 0.02 | 7.16 ± 0.02 | 5.18 ± 0.01 | 7.20 ± 0.02 | 8.54 ± 0.03 | 8.50 ± 0.03 |
| Tb(III) | 3.59 ± 0.03 | 7.20 ± 0.03 | 3.62 ± 0.01 | 7.18 ± 0.03 | 6.33 ± 0.02 | 9.56 ± 0.03 | 3.64 ± 0.01 | 7.18 ± 0.02 | 8.39 ± 0.02 | 7.94 ± 0.02 | 5.36 ± 0.02 | 7.20 ± 0.03 |
| Dy(III) | 3.60 ± 0.03 | 7.18 ± 0.03 | 3.63 ± 0.02 | 3.59 ± 0.01 | 6.77 ± 0.02 | 7.52 ± 0.02 | 3.64 ± 0.01 | 7.18 ± 0.02 | 4.22 ± 0.01 | 7.18 ± 0.02 | 7.50 ± 0.03 | 11.66 ± 0.04 |

[a] $I$ = 0.1 mol·dm$^{-3}$ $KNO_3$ and at 25 °C. [b] ± Refers to three times standard deviation.

$$(M)p(NU)q(H)s + r(NAA) \rightleftharpoons (M)p(NU)q(H)s(NAA)r \quad (3)$$

The second mechanism is the simultaneous type where both the ligand molecules react at the same time with the lanthanide metal ion as depicted in the following equilibrium

$$p\mathrm{M} + q(\mathrm{NU}) + s\mathrm{H} + r(\mathrm{NAA}) \rightleftharpoons (\mathrm{M})p(\mathrm{NU})q(\mathrm{H})s(\mathrm{NAA})r \quad (4)$$

where $p$, $q$, $r$, and $s$ are the number of moles of M, NU, NAA, and H in the formed ternary complex.

All side reactions due to metal hydrolysis for lanthanide metal ions[45−47] have been included in the calculations.

***Spectrophotometric and Fluorometric Measurements.*** The ultraviolet (UV) spectra of the solutions of the binary and ternary complexes were scanned on a Shimadzu spectrophotometer (Shimadzu-1601 pc-UV-Visible automatic recording spectrophotometer with a 1-cm quartz cell). The required volume of the stock metal ion salt is mixed with that of the ligand solution, keeping the total concentration of each solution adjusted to 0.1 mol·dm$^{-3}$ $KNO_3$. All the studied solutions are diluted with bidistilled water, after pH adjustment to the required value using diluted solutions of either $HNO_3$ or KOH. The binary complex solutions in a 1:1 ratio were scanned against bidistilled water as a blank in a 1 cm quartz cell.

The ternary complex solutions were prepared in a 1:1:1 ratio keeping the concentration of each species at $1 \cdot 10^{-5}$ mol·dm$^{-3}$. The desired pH is adjusted to the required value using $HNO_3$ or KOH solutions. Each ternary complex solution was scanned against the corresponding binary complex.

***Spectrofluorometric Measurements.*** The fluorescence spectra of the binary and ternary complexes of Eu(III) and Tb(III)−*N*-acetylamino acids or nucleotides were measured in the same solvent and at the same concentration keeping it at $1 \cdot 10^{-5}$ mol·dm$^{-3}$ and at (25 ± 0.1) °C. The spectra were acquired using a FP-6300 spectrofluorometer with a xenon lamp.

## Results and Discussion

The structures of the studied ligands are shown in Scheme 1. The proton dissociation constants were determined at (25.0 ± 0.1) °C for the studied nucleotides 5′-GMP (HL) (9.44 ± 0.02), 5′-IMP (HL) (9.09 ± 0.03), 5′-AMP (HL) (6.15 ± 0.02), ($H_2L$) (3.8 ± 0.01), 5′-CMP (HL) (6.19 ± 0.03), ($H_2L$) (4.33 ± 0.02), ATP (HL) (6.38 ± 0.02), ($H_2L$) (3.99 ± 0.04), CTP (HL) (6.42 ± 0.02), ($H_2L$) (4.47 ± 0.02), and ADP (HL) (6.3 ± 0.02), ($H_2L$) (3.88 ± 0.02), and the values are in good agreement with those found in the literature.[48]

The deprotonation constant values for the *N*-acetylamino acids were estimated to be for *N*-acetylaspartic acid (HL) (4.49 ± 0.02), ($H_2L$) (3.04 ± 0.02) *N*-acetylglutamic (HL) (4.6 ± 0.02), ($H_2L$) (3.29 ± 0.01) *N*-acetylhistamine (HL) (7.12 ± 0.03), *N*-acetylhistidine (HL) (7.07 ± 0.03), ($H_2L$) (9.92 ± 0.03), *N*-acetyllysine (HL)(10.4 ± 0.03), and *N*-acetylleucine (HL) (9.58 ± 0.04). The obtained values are in good agreement with the literature.[49]

The stability constants of the binary complexes including lanthanide metal ions with nucleotides or *N*-acetylamino acids in a 1:1 and 2:1 ratio were determined from the titration curves. The plus/minus values refer to statistically determined uncertainties at 95 % confidence intervals of the reported values. Tables 1 to 8 illustrate the values of the refined stability constants of all the binary and ternary complexes formed in solution.

Calculation of *p*M for metal-ion buffers containing excess of complexing agent is straightforward,[50] using Schwarzenbach's[51] α-coefficient method. It is necessary to know the pH of the solution, the p$K_a$ values of the ligand, and the stability constants of the metal complexes. If the metal ion undergoes significant hydrolysis, as in our case Ln(III), the appropriate constants are also included.

Stability constants ($\beta'_n$) are defined in terms of the equilibrium between a metal complex and its components, except that the free ligand concentration is replaced by total concentration of all ligand species not actually complexed to the metal, and the free metal ion term includes the hydrolyzed metal ion and the metal ion bound to other complexing species. Calculation of ($\beta'_n$) can be done by

$$\beta'_n = \beta/\alpha_M \cdot (\alpha_L)^n$$

where

$$\alpha_M = ([M] + [MOH] + [M(OH)_2] + ...)/[M]$$

Many metal ions hydrolyze to form polynuclear species so that $\alpha_M$ would be concentration-dependent, but in the presence of an excess of strong ligand it is usually sufficient to consider only the formation of mononuclear species. Under these conditions, $\alpha_M$ reduced to

$$\alpha_M = 1 + 10^{(pH-pK1)} + 10^{(2pH-pK1-pK2)} + ...$$

where p$K_1$, p$K_2$, ... are the successive p$K_a$ values for the loss of a proton from a hydrated metal ion. The metal ion hydrolysis

**Table 3. Formation Constants for La(III) + *N*-Acetylamino Acids + Nucleotide Ternary Complexes in 1:1:1 Ratio[a,b]**

| | *N*-acetylaspartic acid | *N*-acetylglutamic acid | *N*-acetylhistidine | *N*-acetylhistamine | *N*-acetylleucine | *N*-acetyllysine |
|---|---|---|---|---|---|---|
| nucleotide | log $K_{M(NU)(NAA)}$ | log $K_{M(NU)(NAA)}$ | log $K_{M(NU)(NAA)}$ | log $K_{M(NU)(NAA)}$ | log $K_{M(NU)(NAA)}$ | log $K_{M(NU)(NAA)}$ |
| AMP | $3.62^{st} \pm 0.01$ | $3.77^{st} \pm 0.01$ | $7.83^{st} \pm 0.03$ | $3.61^{mo} \pm 0.01$ | $4.44^{mo} \pm 0.02$ | $6.91^{di} \pm 0.02$ |
| ADP | $9.25^{si} \pm 0.03$ | $9.11^{si} \pm 0.03$ | $8.85^{st} \pm 0.03$ | $3.64^{mo} \pm 0.01$ | $6.59^{st} \pm 0.02$ | $5.29^{di} \pm 0.03$ |
| ATP | $8.00^{si} \pm 0.03$ | $4.88^{st} \pm 0.01$ | $7.39^{st} \pm 0.03$ | 3.64st ± 0.01 | $9.77^{st} \pm 0.03$ | $7.75^{mo} \pm 0.02$ |
| GMP | $3.68^{st} \pm 0.01$ | $3.74^{st} \pm 0.01$ | $5.82^{mo} \pm 0.01$ | $4.10^{mo} \pm 0.01$ | $3.70^{mo} \pm 0.01$ | $3.86^{mo} \pm 0.01$ |
| IMP | $3.60^{st} \pm 0.01$ | $6.41^{st} \pm 0.02$ | $6.41^{st} \pm 0.01$ | $3.89^{mo} \pm 0.01$ | - | - |
| CMP | $3.62^{st} \pm 0.01$ | $3.60^{st} \pm 0.01$ | - | $2.73^{mo} \pm 0.01$ | $5.22^{st} \pm 0.03$ | - |
| CTP | $9.24^{si} \pm 0.03$ | $3.64^{st} \pm 0.01$ | $6.97^{st} \pm 0.02$ | $3.39^{mo} \pm 0.01$ | $8.78^{st} \pm 0.04$ | $9.53^{st} \pm 0.03$ |

[a] $I = 0.1$ mol·dm$^{-3}$ $KNO_3$ and at 25 °C. [b] ± Refers to three times standard deviation. st refers to stepwise mechanism. mo refers to monoprotonated mechanism. si refers to simultaneous mechanism. di refers to diprotonated mechanism.

**Table 4. Formation Constants for Sm(III) + *N*-Acetylamino Acid + Nucleotide Ternary Complexes in 1:1:1 Ratio[a,b]**

| | *N*-acetylaspartic acid | *N*-acetylglutamic acid | *N*-acetylhistidine | *N*-acetylhistamine | *N*-acetylleucine | *N*-acetyllysine |
|---|---|---|---|---|---|---|
| nucleotide | log $K_{M(NU)(NAA)}$ | log $K_{M(NU)(NAA)}$ | log $K_{M(NU)(NAA)}$ | log $K_{M(NU)(NAA)}$ | log $K_{M(NU)(NAA)}$ | log $K_{M(NU)(NAA)}$ |
| AMP | $4.96^{di} \pm 0.01$ | $3.91^{st} \pm 0.01$ | $4.13^{mo} \pm 0.02$ | $4.10^{di} \pm 0.01$ | $5.34^{di} \pm 0.01$ | $6.63^{mo} \pm 0.03$ |
| ADP | $8.27^{si} \pm 0.02$ | $9.28^{si} \pm 0.03$ | $8.09^{mo} \pm 0.03$ | $4.81^{di} \pm 0.01$ | $6.84^{st} \pm 0.02$ | - |
| ATP | $8.94^{si} \pm 0.02$ | $9.24^{si} \pm 0.03$ | $7.92^{st} \pm 0.03$ | $9.45^{si} \pm 0.04$ | $8.23^{st} \pm 0.03$ | $5.25^{mo} \pm 0.02$ |
| GMP | $3.62^{st} \pm 0.01$ | $4.21^{st} \pm 0.01$ | $7.98^{mo} \pm 0.02$ | $6.93^{di} \pm 0.03$ | $8.60^{di} \pm 0.03$ | $7.57^{di} \pm 0.02$ |
| IMP | $3.61^{st} \pm 0.01$ | $3.61^{st} \pm 0.01$ | $6.80^{mo} \pm 0.01$ | $3.64^{mo} \pm 0.02$ | $6.76^{di} \pm 0.03$ | - |
| CMP | $4.08^{di} \pm 0.01$ | $3.60^{st} \pm 0.01$ | $8.57^{st} \pm 0.02$ | $4.08^{di} \pm 0.01$ | $4.12^{di} \pm 0.01$ | $7.06^{di} \pm 0.03$ |
| CTP | $3.66^{st} \pm 0.01$ | $3.92^{st} \pm 0.01$ | $7.40^{st} \pm 0.02$ | $4.14^{di} \pm 0.01$ | $7.35^{st} \pm 0.03$ | $7.91^{st} \pm 0.03$ |

[a] $I = 0.1$ mol·dm$^{-3}$ $KNO_3$ and at 25 °C. [b] ± Refers to three times standard deviation. st refers to stepwise mechanism. mo refers to monoprotonated mechanism. si refers to simultaneous mechanism. di refers to diprotonated mechanism.

**Table 5. Formation Constants for Eu(III) + *N*-Acetylamino Acid + Nucleotide Ternary Complexes in 1:1:1 Ratio[a,b]**

| | *N*-acetylaspartic acid | *N*-acetylglutamic acid | *N*-acetylhistidine | *N*-acetylhistamine | *N*-acetylleucine | *N*-acetyllysine |
|---|---|---|---|---|---|---|
| nucleotide | log $K_{M(NU)(NAA)}$ | log $K_{M(NU)(NAA)}$ | log $K_{M(NU)(NAA)}$ | log $K_{M(NU)(NAA)}$ | log $K_{M(NU)(NAA)}$ | log $K_{M(NU)(NAA)}$ |
| AMP | $9.28^{si} \pm 0.03$ | $3.71^{st} \pm 0.01$ | $5.92^{st} \pm 0.02$ | $4.16^{di} \pm 0.02$ | $6.54^{mo} \pm 0.02$ | $8.00^{st} \pm 0.03$ |
| ADP | $6.30^{mo} \pm 0.02$ | $4.71^{mo} \pm 0.01$ | $4.11^{mo} \pm 0.01$ | $3.74^{mo} \pm 0.02$ | $8.37^{di} \pm 0.03$ | $4.24^{mo} \pm 0.02$ |
| ATP | $4.47^{st} \pm 0.01$ | $9.80^{si} \pm 0.03$ | $8.95^{st} \pm 0.03$ | $4.23^{st} \pm 0.02$ | $9.24^{st} \pm 0.03$ | $8.13^{mo} \pm 0.03$ |
| GMP | $3.61^{st} \pm 0.01$ | $3.90^{st} \pm 0.01$ | $6.67^{st} \pm 0.03$ | $3.75^{st} \pm 0.01$ | $6.54^{mo} \pm 0.02$ | $4.53^{st} \pm 0.02$ |
| IMP | $3.6^{mo} \pm 0.01$ | $3.62^{st} \pm 0.01$ | $5.49^{di} \pm 0.02$ | - | $7.41^{mo} \pm 0.02$ | - |
| CMP | $4.29^{di} \pm 0.02$ | $4.19^{di} \pm 0.01$ | $5.61^{mo} \pm 0.02$ | $4.13^{di} \pm 0.02$ | $4.17^{di} \pm 0.03$ | $8.28^{st} \pm 0.04$ |
| CTP | $3.66^{mo} \pm 0.01$ | $4.30^{mo} \pm 0.02$ | $5.18^{st} \pm 0.02$ | $3.61^{st} \pm 0.02$ | $10.74^{mo} \pm 0.03$ | $9.32^{si} \pm 0.04$ |

[a] $I = 0.1$ mol·dm$^{-3}$ $KNO_3$ and at 25 °C. [b] ± Refers to three times standard deviation. st refers to stepwise mechanism. mo refers to monoprotonated mechanism. si refers to simultaneous mechanism. di refers to diprotonated mechanism.

**Table 6. Formation Constants for Gd(III) + *N*-Acetylamino Acid + Nucleotide Ternary Complexes in 1:1:1 Ratio[a,b]**

| | *N*-acetylaspartic acid | *N*-acetylglutamic acid | *N*-acetylhistidine | *N*-acetylhistamine | *N*-acetylleucine | *N*-acetyllysine |
|---|---|---|---|---|---|---|
| nucleotide | log $K_{M(NU)(NAA)}$ | log $K_{M(NU)(NAA)}$ | log $K_{M(NU)(NAA)}$ | log $K_{M(NU)(NAA)}$ | log $K_{M(NU)(NAA)}$ | log $K_{M(NU)(NAA)}$ |
| AMP | - | $3.61^{st} \pm 0.01$ | $3.70^{mo} \pm 0.01$ | $4.10^{di} \pm 0.02$ | $3.60^{mo} \pm 0.02$ | $4.34^{di} \pm 0.02$ |
| ADP | $3.76^{st} \pm 0.01$ | $4.20^{st} \pm 0.02$ | $7.65^{st} \pm 0.02$ | $4.03^{st} \pm 0.02$ | - | $4.28^{di} \pm 0.02$ |
| ATP | $9.10^{si} \pm 0.03$ | $7.42^{si} \pm 0.03$ | $5.90^{st} \pm 0.02$ | $3.53^{st} \pm 0.01$ | $5.54^{st} \pm 0.02$ | $10.59^{mo} \pm 0.03$ |
| GMP | $3.85^{st} \pm 0.02$ | $3.68^{st} \pm 0.01$ | $5.99^{st} \pm 0.02$ | $4.56^{mo} \pm 0.02$ | $5.38^{mo} \pm 0.02$ | – |
| IMP | $3.60^{st} \pm 0.01$ | $4.62^{st} \pm 0.02$ | $6.52^{st} \pm 0.02$ | $4.26^{di} \pm 0.02$ | - | $9.17^{mo} \pm 0.03$ |
| CMP | $4.99^{mo} \pm 0.02$ | $4.08^{di} \pm 0.02$ | $3.79^{mo} \pm 0.01$ | $4.16^{di} \pm 0.02$ | $3.60^{mo} \pm 0.01$ | $5.22^{di} \pm 0.02$ |
| CTP | $4.14^{mo} \pm 0.02$ | $3.97^{st} \pm 0.01$ | - | $9.74^{st} \pm 0.04$ | $8.74^{st} \pm 0.04$ | $9.84^{mo} \pm 0.03$ |

[a] $I = 0.1$ mol·dm$^{-3}$ $KNO_3$ and at 25 °C. [b] ± Refers to three times standard deviation. st refers to stepwise mechanism. mo refers to monoprotonated mechanism. si refers to simultaneous mechanism. di refers to diprotonated mechanism.

**Table 7. Formation Constants for Tb(III) + *N*-Acetylamino Acid + Nucleotide Ternary Complexes in 1:1:1 Ratio[a,b]**

| | *N*-acetylaspartic acid | *N*-acetylglutamic acid | *N*-acetylhistidine | *N*-acetylhistamine | *N*-acetylleucine | *N*-acetyllysine |
|---|---|---|---|---|---|---|
| nucleotide | log $K_{M(NU)(NAA)}$ | log $K_{M(NU)(NAA)}$ | log $K_{M(NU)(NAA)}$ | log $K_{M(NU)(NAA)}$ | log $K_{M(NU)(NAA)}$ | log $K_{M(NU)(NAA)}$ |
| AMP | $3.67^{st} \pm 0.01$ | $3.73^{mo} \pm 0.01$ | $7.65^{mo} \pm 0.03$ | $4.10^{di} \pm 0.02$ | $4.08^{di} \pm 0.02$ | $7.11^{st} \pm 0.03$ |
| ADP | $4.28^{st} \pm 0.02$ | $4.11^{st} \pm 0.02$ | $4.07^{di} \pm 0.02$ | $3.68^{mo} \pm 0.01$ | - | $5.06^{di} \pm 0.02$ |
| ATP | $4.06^{mo} \pm 0.02$ | $4.20^{di} \pm 0.02$ | $6.22^{mo} \pm 0.01$ | - | $10.81^{mo} \pm 0.04$ | − |
| GMP | $4.15^{st} \pm 0.02$ | $8.07^{st} \pm 0.03$ | $8.53^{di} \pm 0.03$ | $5.98^{mo} \pm 0.03$ | - | - |
| IMP | $7.63^{st} \pm 0.03$ | $3.61^{mo} \pm 0.01$ | $4.89^{st} \pm 0.02$ | - | $6.63^{mo} \pm 0.03$ | - |
| CMP | $5.72^{st} \pm 0.02$ | $4.29^{di} \pm 0.02$ | $7.14^{mo} \pm 0.03$ | $4.12^{di} \pm 0.02$ | - | - |
| CTP | $3.69^{st} \pm 0.01$ | $4.12^{mo} \pm 0.01$ | $9.35^{mo} \pm 0.03$ | $4.23^{st} \pm 0.02$ | $10.06^{mo} \pm 0.04$ | $7.17^{st} \pm 0.03$ |

[a] $I = 0.1$ mol·dm$^{-3}$ $KNO_3$ and at 25 °C. [b] ± Refers to three times standard deviation. st refers to stepwise mechanism. mo refers to monoprotonated mechanism. si refers to simultaneous mechanism. di refers to diprotonated mechanism.

**Table 8. Formation Constants for Dy(III) + *N*-Acetylamino Acid + Nucleotide Ternary Complexes in 1:1:1 Ratio[a,b]**

| | *N*-acetylaspartic acid | *N*-acetylglutamic acid | *N*-acetylhistidine | *N*-acetylhistamine | *N*-acetylleucine | *N*-acetyllysine |
|---|---|---|---|---|---|---|
| nucleotide | log $K_{M(NU)(NAA)}$ | log $K_{M(NU)(NAA)}$ | log $K_{M(NU)(NAA)}$ | log $K_{M(NU)(NAA)}$ | log $K_{M(NU)(NAA)}$ | log $K_{M(NU)(NAA)}$ |
| AMP | $9.26^{si} \pm 0.03$ | $3.76^{st} \pm 0.01$ | $7.57^{mo} \pm 0.03$ | $4.11^{di} \pm 0.01$ | $3.60^{mo} \pm 0.01$ | $8.00^{mo} \pm 0.03$ |
| ADP | $3.69^{st} \pm 0.01$ | $4.03^{st} \pm 0.02$ | $7.61^{mo} \pm 0.02$ | $4.24^{di} \pm 0.01$ | $4.79^{mo} \pm 0.02$ | $9.53^{st} \pm 0.04$ |
| ATP | $4.63^{mo} \pm 0.01$ | $9.28^{si} \pm 0.03$ | $9.23^{mo} \pm 0.03$ | $3.61^{mo} \pm 0.01$ | $8.98^{st} \pm 0.03$ | $5.59^{di} \pm 0.02$ |
| GMP | $3.63^{st} \pm 0.01$ | $3.71^{mo} \pm 0.01$ | $8.18^{mo} \pm 0.03$ | $4.28^{di} \pm 0.02$ | $3.62^{mo} \pm 0.01$ | - |
| IMP | $3.60^{st} \pm 0.01$ | $3.76^{st} \pm 0.01$ | $6.80^{mo} \pm 0.02$ | $4.10^{di} \pm 0.02$ | $4.87^{di} \pm 0.02$ | - |
| CMP | $3.60^{st} \pm 0.01$ | $3.62^{mo} \pm 0.01$ | $7.40^{mo} \pm 0.03$ | $4.28^{di} \pm 0.02$ | $4.75^{di} \pm 0.02$ | $5.93^{di} \pm 0.02$ |
| CTP | $6.13^{si} \pm 0.02$ | $4.03^{mo} \pm 0.02$ | $9.01^{mo} \pm 0.04$ | $3.75^{mo} \pm 0.01$ | $7.96^{st} \pm 0.03$ | $9.53^{mo} \pm 0.03$ |

[a] $I = 0.1$ mol·dm$^{-3}$ $KNO_3$ and at 25 °C. [b] ± Refers to three times standard deviation. st refers to stepwise mechanism. mo refers to monoprotonated mechanism. si refers to simultaneous mechanism. di refers to diprotonated mechanism.

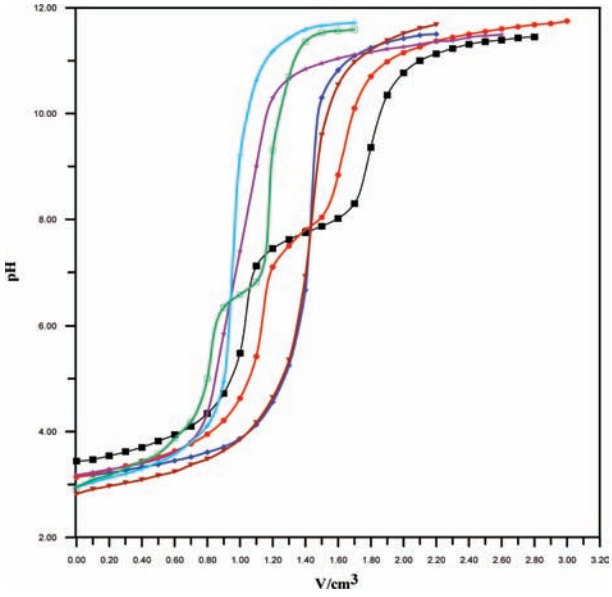


**Figure 1.** pH against volume of 0.0125 mol·dm$^{-3}$ KOH at $I = 0.1$ mol·dm$^{-3}$ $KNO_3$ and $t = (0.25 \pm 0.1)$ °C for Sm(III) + *N*-acetylaspartic + ATP. ◆, $2 \cdot 10^{-3}$ mol·dm$^{-3}$ $HNO_3 + 5 \cdot 10^{-4}$ mol·dm$^{-3}$ *N*-acetylaspartic; ●, $2 \cdot 10^{-3}$ mol·dm$^{-3}$ $HNO_3 + 5 \cdot 10^{-4}$ mol·dm$^{-3}$ *N*-acetylaspartic + $5 \cdot 10^{-3}$ mol·dm$^{-3}$ Sm(III) (binary complex); ★, $2 \cdot 10^{-3}$ mol·dm$^{-3}$ $HNO_3 + 5 \cdot 10^{-4}$ mol·dm$^{-3}$ ATP; +, $2 \cdot 10^{-3}$ mol·dm$^{-3}$ $HNO_3 + 5 \cdot 10^{-4}$ mol·dm$^{-3}$ ATP + Sm(III) (binary complexes); ▼, $2 \cdot 10^{-3}$ mol·dm$^{-3}$ $HNO_3 + 5 \cdot 10^{-4}$mol·dm$^{-3}$ *N*-acetylaspartic + $5 \cdot 10^{-4}$ mol·dm$^{-3}$ ATP + Sm(III) (ternary complexes); □, $2 \cdot 10^{-3}$ mol·dm$^{-3}$ $HNO_3 + 5 \cdot 10^{-4}$ mol·dm$^{-3}$ ATP + $1 \cdot 10^{-3}$ mol·dm$^{-3}$ Sm(III) (dinuclear complex); ■, $2 \cdot 10^{-3}$ mol·dm$^{-3}$ $HNO_3$ + $5 \cdot 10^{-3}$ mol·dm$^{-3}$ *N*-acetylaspartic acid·$10^{-3}$ mol·dm$^{-3}$ Sm(III) (dinuclear complex).

constants published in the IUPAC stability constants database and other sources have been used. [51,52]

All the possible hydrolytic species resulting from the formation of the different hydroxyl complexes including metal ions have been taken into consideration during the SUPERQUAD[44] calculations. Initial estimates of the stability constants of different normal and protonated binary and ternary complexes formed in solution have been refined with the SUPERQUAD[44] computer program. The quality of the fit during this refinement was judged by the values of the sample standard deviations and goodness of fit $\chi^2$ (Pearson's test).

At $\sigma_E = 0.1$ mV (0.001 pH error) and $\sigma_V = 0.005$ mL, the values of the $\sigma$ in different sets of titrations were between 1.0 and 1.7, and $\chi^2$ was between 12.0 and 13.0. The scatter of residuals ($E_{obs} - E_{calc}$) versus pH was reasonably random, without any significant systematic trends, thus indicating a good fit of the experimental data of the expected model systems under our experimental conditions taking into consideration all the possible hydrolysis processes taking part at different pH values.

***Formation Constants of Mono- and Dinuclear Lanthanide Metal Ion Complexes through Potentiometric Measurements.*** The formation constants of Ln(III)−nucleotide binary complexes are collected in Table 1. As indicated in the table, the calculated values of the formation constants of the complexes containing $Sm^{3+}$ have relatively high stability for the 1:1 type with 5′-GMP, 5′-IMP, and 5′-AMP. Table 2 also includes the formation constants of the dimeric species (metal to ligand ratio 2:1). $Sm^{3+}$ gives a relatively high stable dinuclear form with 5′-IMP, 5′-AMP, and 5′-ADP. $Dy^{3+}$ forms also relatively high stable complexes especially in the case of the 5′-GMP molecule. Preferential formation of $Tb^{3+}$−CTP and $Dy^{3+}$−CMP dinuclear complexes is clearly observed with the high formation constants of the dinuclear complexes compared to mononuclear species which may be attributed to that the trivalent metal ions are in close proximity which is in contrary to the lanthanide complexes containing macrocyclic ligands.[53]

Table 2 depicts the formation constants of Ln(III)−*N*-acetylamino acids in their monomeric and dimeric forms. The interaction of *N*-acetylglutamic acid with the lanthanide metal ions gives corresponding binary complexes of little difference in their stability constants either in 1:1 or 2:1 forms. Dy(III) forms the most stable complex with *N*-acetyllysine in 1:1 form. It is quite interesting to observe that the dinuclear form of the Tb(III)−*N*-acetylhistidine binary complex exhibits the most stable complex among the dimeric forms of the lanthanide metal ions with *N*-acetylhistidine. As the lanthanide ion Tb(III) possesses long-lived excited states, which can be populated by

sensitizing *N*-acetylhistidine antennae, and emit at long wavelengths in the visible region, these are particularly desirable features for sensing as it overcomes drawbacks such as light scattering and auto fluorescence associated with short wavelength emitting sensors. Also, *N*-acetylhistamine gives approximately the same values of stability constants of its complexes with the lanthanide metal ions. Eu(III) and Tb(III) are two of the versatile lanthanide metal ions since they exhibit promising high stable complexes with *N*-acetylleucine (log $K$ = 9.33 ± 0.03 and 8.39 ± 0.02). *N*-Acetyllysine is a high probable amino acid for chelation of Gd(III) and Dy(III). The dinuclear forms $(Eu)_2$−*N*-acetyllysine and $(Dy)_2$−*N*-acetyllysine are highly stable complexes.

***Ternary Complexes Containing La(III).*** During our SUPERQUAD calculations, *N*-acetyllysine has been considered as the secondary ligand attacking the binary complex La(III)−CTP to form the highly stable ternary complex species (log $K$ = 9.53 ± 0.04) in a stepwise manner. The low basicity of *N*-acetylhistamine reflects itself on the somewhat low stability of La−ATP−*N*-acetylhistamine (log $K$ = 3.64 ± 0.02); on the other hand, the mixed ligand complex including *N*-acetylleucine exhibits high stability (log $K$ = 9.77 ± 0.03).

***Ternary Complexes Containing Sm(III).*** *N*-Acetylglutamic acid gives higher stability ternary complex species with Sm(III)−ATP (log $K$ = 9.24 ± 0.03) than *N*-acetylaspartic acid (log $K$ = 8.94 ± 0.03), and the reaction proceeds in a simultaneous mechanism as shown in Figure 1. The stepwise mechanism is the predominant one in formation of different complex species indicating Sm−CMP−*N*-acetylhistidine, Sm(III)−CTP−*N*-acetyllysine, and Sm(III)−ATP−*N*-acetylleucine. The presence of more than two inflections in some titration curves can be attributed to the different tendencies of the lanthanide metal ions, based on their lewis bascities, to form polymeric complexes at different pH ranges. This behavior has been confirmed by the models considered during SUPERQUAD calculations.

***Ternary Complexes Containing Eu(III).*** Eu(III) reacts readily with the adenine nucleotide forming relatively stable complexes which then interact with *N*-acetylaspartic acid, *N*-acetylhistidine, and *N*-acetylglutamic to form complex species with stability constant values of (log $K$ = 9.28 ± 0.03, 8.95 ± 0.03, and 9.80 ± 0.03), respectively.

As previously discussed, the higher value of the formation constant for Eu(III)−CTP−*N*-acetyllysine (log $K$ = 9.32 ± 0.03) may be attributed to the participation of the amino group of *N*-acetyllysine in the formation of the ternary complexes which reflect the great degree of probability of formation of a stable complex.

The ternary complex Eu(III)−ATP−*N*-acetylleucine begins to form at pH > 5.5 as indicated in Figure 2 where the amino acid ligand interacts with the Eu(III)−ATP binary complex to form the ternary complex (log $K$ = 9.24 ± 0.03), while in the case of *N*-acetylhistamine the mixed ligand complex including Eu(III)−ATP with this amino acid has relatively lower stability (log $K$ = 4.23 ± 0.03). This result can be attributed to the lower basicity of the amino acid (*N*-acetylhistamine).

***Ternary Complexes Containing Gd(III).*** The data which are collected in Table 6 indicate that Gd(III) interacts with the ATP molecule and either *N*-acetylaspartic acid or *N*-acetylglutamic acid simultaneously to form mixed ligand complexes of stability constant log $K$ = 9.10 ± 0.03 and 7.42 ± 0.03, respectively, with the lower stability constant value of the ternary complex containing *N*-acetylglutamic acid attributed to the presence of the $\sigma$-COOH group in the ligand.

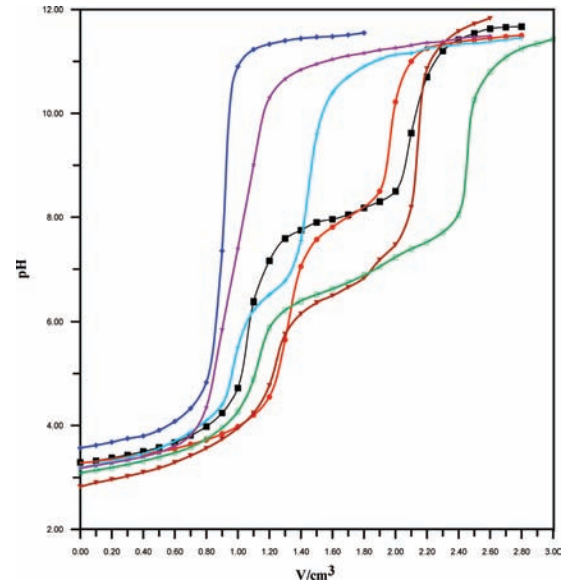


**Figure 2.** pH against volume of 0.0125 mol·dm$^{-3}$ KOH at $I$ = 0.1 mol·dm$^{-3}$ $KNO_3$ and $t$ = (0.25 ± 0.1) °C for Eu(III) + *N*-acetylleucine + ATP. ◆, 2·10$^{-3}$ mol·dm$^{-3}$ $HNO_3$ + 5·10$^{-4}$ mol·dm$^{-3}$ *N*-acetylleucine; ●, 2·10$^{-3}$ mol·dm$^{-3}$ $HNO_3$ + 5·10$^{-4}$ mol·dm$^{-3}$ *N*-acetylleucine + 5·10$^{-3}$ mol·dm$^{-3}$ Eu(III) (binary complex); ★, 2·10$^{-3}$ mol·dm$^{-3}$ $HNO_3$ + 5·10$^{-4}$ mol·dm$^{-3}$ ATP; +, 2·10$^{-3}$ mol·dm$^{-3}$ $HNO_3$ + 5·10$^{-4}$ mol·dm$^{-3}$ ATP + Eu(III) (binary complexes); ▼, 2·10$^{-3}$ mol·dm$^{-3}$ $HNO_3$ + 5·10$^{-4}$mol·dm$^{-3}$ *N*-acetylleucine + 5·10$^{-4}$ mol·dm$^{-3}$ ATP + Eu(III) (ternary complexes); □, 2·10$^{-3}$ mol·dm$^{-3}$ $HNO_3$ + 5·10$^{-4}$ mol·dm$^{-3}$ ATP + 1·10$^{-3}$ mol·dm$^{-3}$ Eu(III) (dinuclear complex); ■, 2·10$^{-3}$ mol·dm$^{-3}$ $HNO_3$ + 5·10$^{-3}$ mol·dm$^{-3}$ *N*-acetylleucine + 1·10$^{-3}$ mol·dm$^{-3}$ Eu(III)(dinuclear complex).

The complex species of Gd(III)−ADP−*N*-acetylhistidine begins to form around pH ≈ 6.5 which indicates the stepwise formation of this complex since the Gd(III)−ADP binary complex is attacked through N-1 of the imidazole moiety of the histidyl amino acid derivative. The probability of the coordination participation of *N*-acetylhistamine as the secondary ligand is greater than that of *N*-acetylhistidine, and this behavior reflects itself through the higher stability constant of Gd(III)−ADP−*N*-acetylhistamine (log $K$ = 9.74 ± 0.03) compared with Gd(III)−ADP−*N*-acetylhistidine (log $K$ = 7.65 ± 0.03).

During our SUPERQUAD calculations, we considered in our model system that *N*-acetylleucine reacts as a secondry ligand with the Gd(III)−CTP binary complex in a stepwise manner, and the complex formation starts at a low pH value ≈ 4.0 forming a relatively stable complex (log $K$ = 8.74 ± 0.03).

***Ternary Complexes Containing Tb(III).*** The purine nucleotides 5′-IMP and 5′-GMP react with great tendencies in stepwise manners with Tb(III)−*N*-acetylaspartic acid and *N*-acetylglutamic acid, respectively, forming two types of highly stable mixed ligand complexes with (log $K$ = 7.63 ± 0.03 and 8.07 ± 0.02), respectively.

The triphosphate pyrimidine nucleotide (CTP) is a promising primary ligand with Tb(III) due to the great probability of chelation through phosphate groups and the oxophilic nature of the studied lanthanide metal ion. The results indicate that *N*-acetyllysine is a preferable secondary ligand which reacts readily with the Tb−CTP binary complex to form a ternary complex with a stability constant value log $K$ = 7.17 ± 0.03. In the present study, we develop new strategies concerning the possible use of Tb(III) cations as spectroscopic probes for the study of molecular structures in biological solutions containing both nucleotides and *N*-acetyl amino acids. The high stability constants obtained for the ternary systems under investigation

**Table 9. Δ log $K_M$ for La(III) + *N*-Acetylamino Acid + Nucleotide Ternary Complexes[a,b,c]**

| nucleotide | *N*-acetylaspartic acid | *N*-acetylglutamic acid | *N*-acetylhistidine | *N*-acetylhistamine | *N*-acetylleucine | *N*-acetyllysine |
|---|---|---|---|---|---|---|
| AMP | $+0.14^{st}$ | $+0.14^{st}$ | $4.17^{st}$ | - | - | - |
| ADP | $+2.24^{si}$ | $+2.24^{si}$ | $5.19^{st}$ | - | $1.91^{st}$ | - |
| ATP | $+0.38^{si}$ | $+1.3^{st}$ | $3.73^{st}$ | $-0.04^{st}$ | $5.09^{st}$ | - |
| GMP | $+0.2^{st}$ | $+0.16^{st}$ | - | - | - | - |
| IMP | $+0.12^{st}$ | $+2.83^{st}$ | $2.75^{st}$ | - | - | -- |
| CMP | $+0.14^{st}$ | $+0.02^{st}$ | - | - | $0.54^{st}$ | - |
| CTP | $+2.16^{si}$ | $+0.06^{st}$ | $3.31^{st}$ | - | $4.1^{st}$ | $4.51^{st}$ |

[a] $I = 0.1$ mol·dm$^{-3}$ $KNO_3$ and at 25 °C. [b] $\Delta \log K_M^{st} = \log K_{M(NU)(NAA)}^{M(NU)} - \log K_{M(NAA)}^{M}$. [c] $\Delta \log K_M^{si} = \log K_{M(NU)(NAA)}^{M} - (\log K_{M(NU)}^{M} + \log K_{M(NAA)}^{M})$.

**Table 10. Δ log $K_M$ for Sm(III) + *N*-Acetylamino Acid + Nucleotide Ternary Complexes[a,b,c]**

| Nucleotide | *N*-acetylaspartic acid | *N*-acetylglutamic acid | *N*-acetylhistidine | *N*-aetylhistamine | *N*-aetylleucine | *N*-aetyllysine |
|---|---|---|---|---|---|---|
| AMP | - | $+0.32^{st}$ | - | - | - | - |
| ADP | $+1.45^{si}$ | $+2.47^{si}$ | - | - | $+2.74^{st}$ | - |
| ATP | $+1.72^{si}$ | $+2.03^{si}$ | $+4.15^{st}$ | $+2.14^{si}$ | $+4.13^{st}$ | - |
| GMP | $+0.02^{st}$ | $+0.62^{st}$ | - | - | - | - |
| IMP | $+0.01^{st}$ | $+0.02^{st}$ | - | - | - | - |
| CMP | - | $+0.01^{st}$ | $+4.8^{st}$ | - | - | - |
| CTP | $+0.06^{st}$ | $+0.33^{st}$ | $+3.63^{st}$ | - | $+3.25^{st}$ | $+1.33^{st}$ |

[a] $I = 0.1$ mol·dm$^{-3}$ $KNO_3$ and at 25 °C. [b] $\Delta \log K_M^{st} = \log K_{M(NU)(NAA)}^{M(NU)} - \log K_{M(NAA)}^{M}$. [c] $\Delta \log K_M^{si} = \log K_{M(NU)(NAA)}^{M} - (\log K_{M(NU)}^{M} + \log K_{M(NAA)}^{M})$.

**Table 11. Δ log $K_M$ for Eu(III) + *N*-Acetylamino Acid + Nucleotide Ternary Complexes[a,b,c]**

| ncleotide | *N*-aetylaspartic acid | *N*-aetylglutamic acid | *N*-aetylhistidine | *N*-aetylhistamine | *N*-aetylleucine | *N*-aetyllysine |
|---|---|---|---|---|---|---|
| AMP | $+2.05^{si}$ | $+0.1^{st}$ | $+2.26^{st}$ | - | - | $1.78^{st}$ |
| ADP | - | - | - | - | - | - |
| ATP | - | $+2.43^{si}$ | $+5.29^{st}$ | $+0.56^{st}$ | $-0.09^{st}$ | - |
| GMP | $+0.02^{st}$ | $+0.29^{st}$ | $+3.01^{st}$ | $+0.08^{st}$ | - | $-1.69^{st}$ |
| IMP | - | $+0.01^{st}$ | - | - | - | - |
| CMP | - | - | - | - | - | $2.06^{st}$ |
| CTP | - | - | $+1.52^{st}$ | $+0.06^{st}$ | - | $3.1^{st}$ |

[a] $I = 0.1$ mol·dm$^{-3}$ $KNO_3$ and at 25 °C. [b] $\Delta \log K_M^{st} = \log K_{M(NU)(NAA)}^{M(NU)} - \log K_{M(NAA)}^{M}$. [c] $\Delta \log K_M^{si} = \log K_{M(NU)(NAA)}^{M} - (\log K_{M(NU)}^{M} + \log K_{M(NAA)}^{M})$.

**Table 12. Δ log $K_M$ for Gd(III) + *N*-Acetylamino Acid + Nucleotide Ternary Complexes[a,b,c]**

| nucleotide | *N*-aetylaspartic acid | *N*-acetylglutamic acid | *N*-acetylhistidine | *N*-acetylhistamine | *N*-acetylleucine | *N*-acetyllysine |
|---|---|---|---|---|---|---|
| AMP | - | $+0.02^{st}$ | - | - | - | - |
| ADP | $+0.15^{st}$ | $+0.61^{st}$ | $+4.01^{st}$ | $+0.43^{st}$ | - | - |
| ATP | $+1.88^{si}$ | $+0.22^{si}$ | $+2.26^{st}$ | $-0.07^{st}$ | $+0.36^{st}$ | - |
| GMP | $+0.24^{st}$ | $+0.09^{st}$ | $+2.35^{st}$ | - | - | - |
| IMP | $-0.01^{st}$ | $+1.03^{st}$ | $+2.88^{st}$ | - | - | - |
| CMP | - | - | - | - | - | - |
| CTP | - | $+0.38^{st}$ | - | $+6.14^{st}$ | $+3.56^{st}$ | - |

[a] $I = 0.1$ mol·dm$^{-3}$ $KNO_3$ and at 25 °C. [b] $\Delta \log K_M^{st} = \log K_{M(NU)(NAA)}^{M(NU)} - \log K_{M(NAA)}^{M}$. [c] $\Delta \log K_M^{si} = \log K_{M(NU)(NAA)}^{M} - (\log K_{M(NU)}^{M} + \log K_{M(NAA)}^{M})$.

indicate that the trial is promising. Biosensors containing Tb(III)−nucleotides as analytes are now under investigation in our laboratory with one of our international collaborators. Also, the interesting luminescent detection of *N*-acetylaspartic acid which is an important metabolite in the human brain using luminescent Tb(III)−nucleotide complexes will be the subject of further investigation in our laboratory. Widespread interest for lanthanides is mainly centered in the fact that systems containing lanthanides enjoy a very favorable situation since these ions feature high coordination numbers, which ensure rich binding chemistry, and at the same time they possess the right spectroscopic properties to monitor it.

***Ternary Complexes Containing Dy(III).*** The interesting feature of the ternary complexes involving Dy(III) is the high stability constants of the species containing the purine nucleotides of the adinine moiety (5′-AMP, 5-ADP, and 5′-ATP). For the dicarboxylic *N*-acetylamino acids (*N*-acetylaspartic and *N*-acetylglutamic), the mechanism of ternary complex formation occurs via a simultaneous type of formation.

***Comparison between Binary and Ternary Complexes Formed.*** The Δ log $K_M$ values for Ln(III) + nucleotide + *N*-acetylamino acid are collected in Tables 9 to 14. The high positive values of Δ log $K_M$ are observed in the case *N*-acetylhistidine for La(III) + NU + NAA for either the stepwise or simultaneous mechanism. For Dy(III) + NU + NAA, the more positive Δ log $K_M$ values are obtained for the *N*-acetylleucine molecule.

In the case of Eu(III) + NU + NAA, the high positive values of Δ log $K_M$ are clearly indicated for *N*-acetylhistidine. Also, the ternary complex including *N*-acetyllysine gives a relatively stable complex with a high probability of formation. For ternary complexes containing Tb(III), *N*-acetylaspartic acid is the most probable attacking secondary ligand toward Tb(III)−nucleotide binary complexes.

CTP is the preferred nucleotide for Tb(III) that easily interacts with *N*-acetyllysine. For the mixed ligand complexes of the type Gd(III)−nucleotide−*N*-acetylamino acid, *N*-acetylhistidine is the most feasible ligand to react with the $Gd^{3+}$ nucleotide. The most characteristic feature for Gd(III) complexes is the high positive Δ log $K_M$ values for Gd(III)−CTP−*N*-acetylhistamine and Gd(III)−CTP−*N*-acetylleucine.

The high positive values for ternary complexes containing Sm(III) are observed for those systems containing *N*-acetylhistidine, where the complex species are formed in a stepwise mechanism. Also, relatively high values are obtained for Sm(III)−ADP, Sm(III)−ATP, or Sm(III)−CTP complexes

**Table 13. Δ log $K_M$ for Tb(III) + *N*-Acetylamino Acid + Nucleotide Ternary Complexes[a,b,c]**

| nucleotide | *N*-acetylaspartic acid | *N*-acetylglutamic acid | *N*-acetylhistidine | *N*-acetylhistamine | *N*-acetylleucine | *N*-acetyllysine |
|---|---|---|---|---|---|---|
| AMP | $+0.08^{st}$ | - | - | - | - | $+1.75^{st}$ |
| ADP | $+0.69^{st}$ | $+0.49^{st}$ | - | - | - | - |
| ATP | - | - | - | - | - | - |
| GMP | $+0.56^{st}$ | $+4.45^{st}$ | - | - | - | - |
| IMP | $+4.04^{st}$ | - | $+0.65^{st}$ | - | - | - |
| CMP | $+2.13^{st}$ | - | - | - | - | - |
| CTP | $+0.1^{st}$ | - | - | $+0.59^{st}$ | - | $+1.81^{st}$ |

[a] $I = 0.1$ mol·dm$^{-3}$ $KNO_3$ and at 25 °C. [b] $\Delta \log K_M^{st} = \log K_{M(NU)(NAA)}^{M(NU)} - \log K_{M(NAA)}^{M}$. [c] $\Delta \log K_M^{si} = \log K_{M(NU)(NAA)}^{M} - (\log K_{M(NU)}^{M} + \log K_{M(NAA)}^{M})$.

**Table 14. Δ log $K_M$ for Dy(III) + *N*-Acetylamino Acid + Nucleotide Ternary Complexes[a,b,c]**

| nucleotide | *N*-acetylaspartic acid | *N*-acetylglutamic acid | *N*-acetylhistidine | *N*-acetylhistamine | *N*-acetylleucine | *N*-acetyllysine |
|---|---|---|---|---|---|---|
| AMP | $+1.86^{si}$ | $+0.13^{st}$ | - | - | - | - |
| ADP | $+0.09^{st}$ | $+0.4^{st}$ | - | - | - | $+2.03^{st}$ |
| ATP | - | $+2.12^{si}$ | - | - | $+4.76^{st}$ | - |
| GMP | $+0.03^{st}$ | - | - | - | - | - |
| IMP | $0.00^{st}$ | $+0.13^{st}$ | - | - | - | - |
| CMP | $0.00^{st}$ | - | - | - | - | - |
| CTP | $-0.86^{si}$ | - | - | - | $+3.74^{st}$ | - |

[a] $I = 0.1$ mol·dm$^{-3}$ $KNO_3$ and at 25 °C. [b] $\Delta \log K_M^{st} = \log K_{M(NU)(NAA)}^{M(NU)} - \log K_{M(NAA)}^{M}$. [c] $\Delta \log K_M^{si} = \log K_{M(NU)(NAA)}^{M} - (\log K_{M(NU)}^{M} + \log K_{M(NAA)}^{M})$.

reacting with *N*-acetylleucine. Also, Sm(III)−CTP reacts preferentially with *N*-acetyllysine and *N*-acetylleucine.

Generally different trends can be obtained for the stability constants of different ternary systems investigated in the present study. Taking into consideration the factors which affect lanthanide nucleotide interactions as well as factors associated with trivalent lanthanide chemistry, one can account for the different trends observed for the stability constants of several ternary complexes of the type Ln(III)−NU−NAA. Via the formation of mixed-ligand complexes, certain ligand−ligand associations and interactions may be favored, and thus distinct structures may be created in a way that involves only small changes from an energetic point of view.

***Ultraviolet Absorption Spectra for the Binary and Ternary Complexes.*** Optical absorption spectra of binary complexes containing Eu(III) and Tb(III) with the nucleotide molecules (5′-GMP, 5′-IMP, 5′-AMP, 5′-CMP, and the enriched energy molecule 5′-ATP) and *N*-acetylamino acids (*N*-acetylhistidine, *N*-acetylaspartic acid, *N*-acetylglutamic acid, and *N*-acetylleucine) have been investigated. The data reveal that the Eu(III)−5′-AMP complex exhibits two well-separated peaks at $\lambda_1$ 210.20 nm and $\lambda_2$ 259.20 nm with nearly equal absorptivity. The first peak may be attributed to a $\pi-\pi^*$ transition in the purine ring, while the second band could be considered due to a $n-\pi^*$ transition.

The $\pi-\pi^*$ transition in the purine ring of the guanine molecule is perturbed and shifted to red, and also the $n-\pi^*$ transition is shifted to a longer wavelength due to the different mode of coordination of Eu(III) with 5′-GMP rather than Eu(III)−5′-AMP. The different structure of the pyrimidine ring reflects itself on the type of transition in the Eu(III)−5′-CMP binary complex, where only one peak is observed at $\lambda$ 274.2 nm and of relatively significant absorption. For the Eu(III)−5′-ATP binary complex, two well-separated peaks are obtained where the first one is located at $\lambda$ 254.6 nm which may be attributed to a $\pi-\pi^*$ transition, and a charge transfer band is observed at 348.4 nm of somewhat low absorptivity.

Eu(III)−*N*-acetylamino acids exhibit the same $\lambda_{max}$ [(252.6 to 254) nm] irrespective of the nature of *N*-acetylamino acid but of different molar absorptivity. The absorbance value can be arranged as follows: *N*-acetylaspartic acid > *N*-acetylhistidine > *N*-acetylglutamic acid > *N*-acetylleucine > *N*-acetylhistamine, with respect to the ligand moiety in the corresponding Eu(III) binary complexes.

The Tb(III)−5′-AMP binary complex acquires the same trend of absorption as the analogues including Eu(III), where two absorption peaks are observed at $\lambda_1$ 210 nm and $\lambda_2$ 261 nm. Also, the two peaks have approximately the same absorptivity, which indicate that the mode of coordination is the same for Eu(III)−5′-AMP and Tb(III)−5′-AMP. On the contrary, for the 5′-GMP molecule, Tb(III)−5′-GMP exhibits only one absorption peak which is located at $\lambda$ 254 nm, and contrary to the Eu(III)−5′-GMP binary complex where this latter species has two absorption peaks, hence the two corresponding complexes have different environments. The pyrimidine molecule 5′-CMP coordinates similarly with Tb(III) and Eu(III), where it exhibits only one absorption peak at $\lambda = 254$ nm. The charge transfer peak which is clearly observed in Eu(III)−5′-ATP is absent in the analogue Tb(III)−5′-ATP molecule, hence the two complexes have different modes of coordination.

*N*-Acetylamino acids upon reacting with Tb(III) acquire only one absorption band at $\lambda$ 256.6 nm but of different molar absorptivity following the order: *N*-acetylhistidine > *N*-acetylleucine > *N*-acetylaspartic acid > *N*-acetyllysine > *N*-acetylhistamine > *N*-acetylhistidine.

Comparing the absorption spectra for the Eu(III) binary complexes with nucleotides or *N*-acetylaspartic acids and the corresponding ternary complexes as depicted in Figure 3a indicates that for the ternary complex of the type Eu(III)−5′-GMP−*N*-acetylaspartic acid the ternary complex acquires a quite different curve where two peaks are observed: the first located at $\lambda$ 195.4 nm, while the second occurs at $\lambda$ 258 nm. This behavior may be explained by the fact that upon formation of the ternary complex the peak is shifted to blue, hence a highly stable complex is produced.

The ternary complex containing Eu(III)−5′-CMP−*N*-acetylaspartic acid as shown in Figure 3b has two small splitted peaks with a shift to red. The decrease in absorbance and the shift in the absorption curve for the ternary complex confirm the formation of quite different complexes rather than the corresponding binary complexes.

The incorporation of 5′-AMP in the ternary system Eu(III)−5′-AMP−*N*-acetylaspartic acid as indicated in Figure 3c results in a great decrease in the absorption of the ternary complex comparing to the spectral peak of the binary complex Eu(III)−5′-AMP. This means that the ternary complex species exhibit different absorption manners due to structural changes.

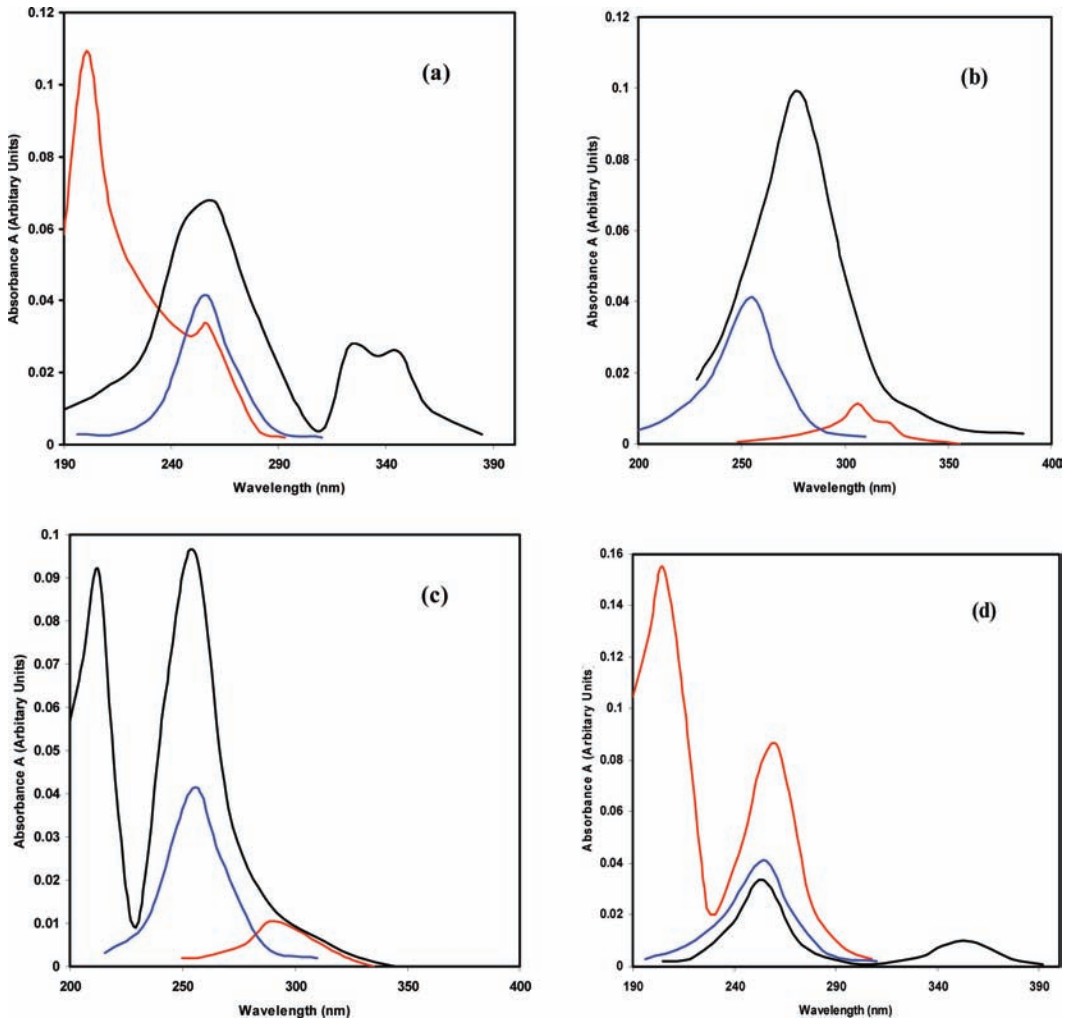


**Figure 3.** UV absorption spectra for the $Eu^{3+}$ + nucleotides + *N*-acetylaspartic acid at $I = 0.1$ mol·dm$^{-3}$ $KNO_3$ and $t = (25.0 \pm 0.1)$ °C, pH = 6.5 to 7.0. Black line, $1 \cdot 10^{-4}$ mol·dm$^{-3}$ $Eu^{3+}$ + $1 \cdot 10^{-4}$ mol·dm$^{-3}$ nucleotide; blue line, $1 \cdot 10^{-4}$ mol·dm$^{-3}$ $Eu^{3+}$ + $1 \cdot 10^{-4}$ mol·dm$^{-3}$ *N*-acetylaspartic acid; red line, $1 \cdot 10^{-4}$ mol·dm$^{-3}$ $Eu^{3+}$ + $1 \cdot 10^{-4}$ mol·dm$^{-3}$ *N*-acetylaspartic acid + $1 \cdot 10^{-4}$ mol·dm$^{-3}$ nucleotide. (a) 5′-GMP. (b) 5′-CMP. (c) 5′-AMP. (d) 5′-ATP.

The most characteristic feature of the ternary complex containing 5′-ATP with Eu(III) and *N*-acetylaspartic acid as indicated in Figure 3d is the blue shift of the absorption peak, where the first peak appears at $\lambda$ 202 nm and the second takes place at $\lambda$ 258 nm, where it means that the absorption peak attributed to Eu(III)−5′-ATP and Eu(III)−*N*-acetylaspartic acid is enhanced upon reacting together to form the ternary complex. A more intense peak is observed at a lower wavelength, hence a high stable complex may probably be formed with log $K$ = 9.26 ± 0.03 and 9.28 ± 0.03 for Dy(III)−5′-AMP−*N*-acetylaspartic acid and Dy(III)−5′-ATP−*N*-acetylglutamic acid, respectively.

A typical comparison of the binary complexes of Tb(III) nucleotides, Tb(III)−*N*-acetylaspartic acid, and the corresponding ternary complexes where each nucleotide molecule exhibits a characteristic behavior toward the lanthanide metal ion linked to the neuro important *N*-acetylamino acid has been investigated (figure is not shown in the text). The two well-separated absorption peaks observed for the Tb(III)−5′-AMP binary complex are contracted in one broad peak of low absorptivity which is slightly shifted from the corresponding Tb(III)−*N*-acetylaspartic binary complex.

In the case of the 5′-GMP nucleotide molecule, the binary Tb(III)−5′-GMP complex has a considerable high absorbance in comparison to Tb(III)−*N*-acetylaspartic acid, the mixed ligand complex containing the purine nucleotide, and the amino acid molecule acquires slightly higher intensity than the binary Tb(III)−*N*-acetylaspartic acid. The substantial decrease in absorbance of Tb(III)−5′-GMP upon formation of the ternary complex indicates that 5′-GMP can be considered as the primary ligand, while *N*-acetylaspartic acid acts as a secondary ligand with Eu(III)−5′-GMP. This behavior can be attributed to the high tendency of Eu(III) ions toward the coordination with the phosphate groups of 5′-GMP.

The absorbance of the mixed ligand complex Tb(III)−5′-CMP−*N*-acetylaspartic acid is shifted toward a longer wavelength compared to that of the corresponding Tb(III)−5′-CMP and Tb(III)−*N*-acetylaspartic acid, which may be attributed to the participation of the main acid moiety in the coordination sphere during the formation of the ternary complex, which may result in a reduction of the energy required for this molecule to absorb.

The two binary complexes Tb(III)−5′-ATP and Tb(III)−*N*-acetylamino acid absorb in the range of $\lambda$ = (250 to 260) nm, where the binary complex including the 5′-ATP molecule has a high absorbance value with regard to the corresponding binary complex Tb(III)−*N*-acetylaspartic acid. The ternary complex acquires a slight increase in the absorbance peak of the binary Tb(III)−*N*-acetylaspartic acid, where also the formation of the

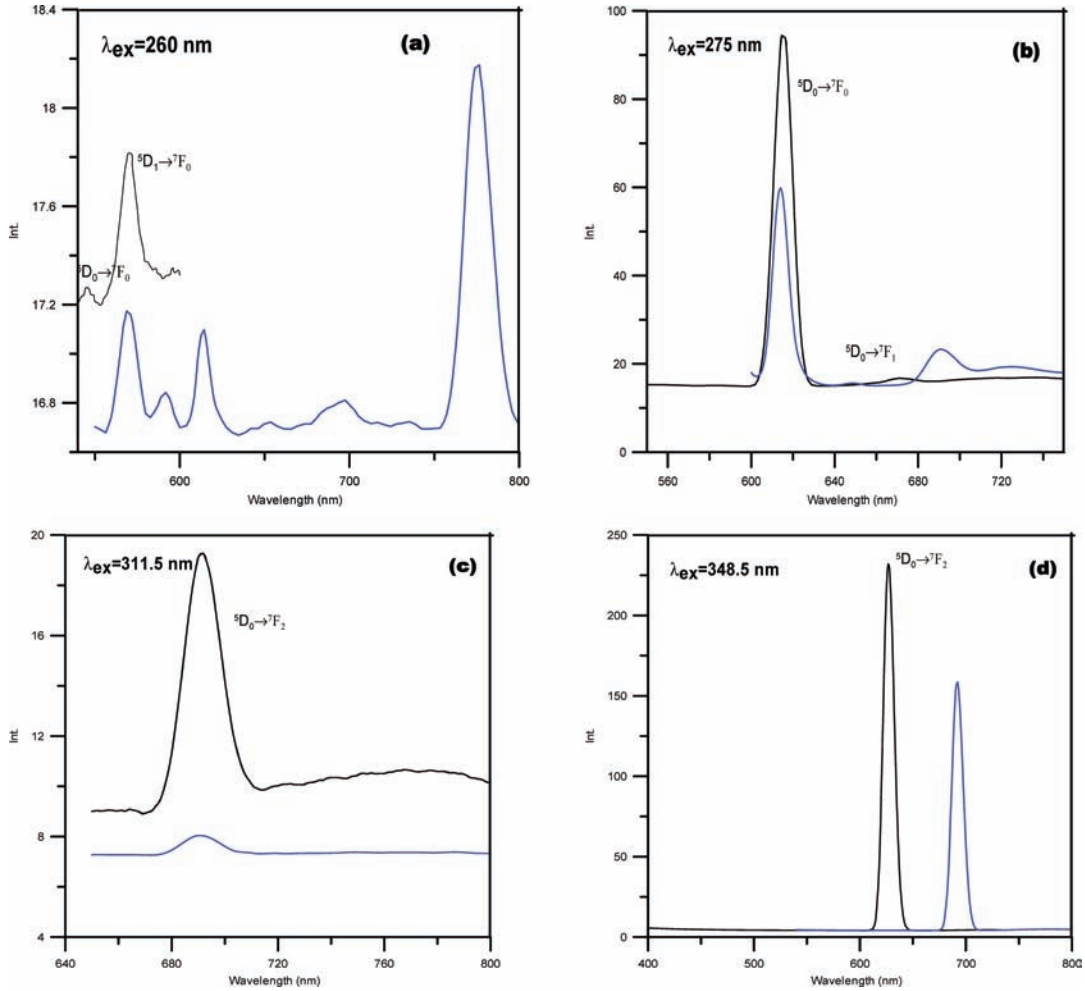


**Figure 4.** Emission spectra for $Eu^{3+}$−nucleotide (NU) binary complexes at $t = (25.0 \pm 0.1)$ °C, pH = 6.5 to 7.0, $[Eu^{3+}] = [NU] = 1 \cdot 10^{-5}$ mol·dm$^{-3}$. (a) 5′-AMP. (b) 5′-CMP. (c) 5′-GMP. (d) 5′-ATP. Black line, $Eu^{3+}$−nucleotide binary complex; blue line, nucleotide free ligand.

ternary complex occurs via the reaction of Tb(III)−5′-ATP with *N*-acetylaspartic acid to form the ternary complex.

Luminescent lanthanide chelate complexes have unusual spectral characteristics when compared to typical organic fluorophores. These include millisecond lifetimes, sharply spiked emission spectra, high quantum yield, unpolarized emission, and a broad range of emission energies extending from the blue to the red part of the spectrum. Lanthanides are therefore an alternative to organic fluorophores particularly where there are problems of background autofluorescence[54,55] and as donors in fluorescence (luminescence) resonance energy transfer to measure nanometer conformational changes and binding events within proteins.[56−58]

The importance of these complexes is critical when containing a chelate which serves several purposes, including binding the lanthanide tightly, shielding the lanthanide ion from the quenching effect of water, and acting as a scaffold for attachment of the antenna and a reactive group which facilitate the coupling of the chelate complex to biomolecules.

***Emission Spectra for Eu(III) Complexes.*** Figure 4 depicts the emission spectra for Eu(III)−nucleotide binary complexes, whereas, shown in the figure, the four types of nucleotides used 5′-AMP, 5′-GMP, 5′-CMP, and 5′-ATP with Eu(III) metal ions are compared with the free ligands. For the first three nucleotides (5′-AMP, 5′-CMP, and 5′-GMP) the corresponding binary complexes acquire the same emission bands but of higher intensity. Such emission peaks could be attributed to $^5D_0\rightarrow{}^7F_0$ and $^5D_0\rightarrow{}^7F_1$ transitions for the Eu(III)−5′-AMP binary complex. Only one emission peak is obtained for Eu(III)−5′-GMP which could be assigned to a $^5D_0\rightarrow{}^7F_2$ transition. The $^5D_0\rightarrow{}^7F_2$ is the characteristic transition type for the Eu(III)−5′-CMP binary complex.

The most interesting feature is the observed considerable enhancement in the emission peak intensity of Eu(III)−5′-CMP compared to that of the free ligand (about 35 au). Such an increase is less considerable for Eu(III)−5′-GMP (about 11 au). There is a very low slight increase in intensity of Eu(III)−5′-AMP which is only higher than that of the free ligand 5′-AMP by a small fraction of 0.06 au.

The binding of Eu(III) to the 5′-ATP molecule is characterized by an emission band at $\lambda$ 622 nm which is attributed to the $^5D_0\rightarrow{}^7F_2$ transition. The free ligand 5′-ATP exhibits an emission band at $\lambda$ 692 nm, where it could be concluded that there is energy transfer from the Eu(III) f-electrons to the nucleotide molecule.

The emission spectra for Eu(III) with the two *N*-acetylamino acids containing an imidazole ring are depicted in Figure 5. Eu(III)−*N*-acetylhistidine acquires two emission bands at 557 nm which could be assigned to a $^5D_0\rightarrow{}^7F_0$ transition and at 757 nm which may be attributed to a $^5D_0\rightarrow{}^7F_5$ transition. The emission band appearing at 754 nm for the free ligand *N*-acetylhistidine is enhanced upon coordination with Eu(III), and such an increase in emission intensity could be explained by the transfer of energy from

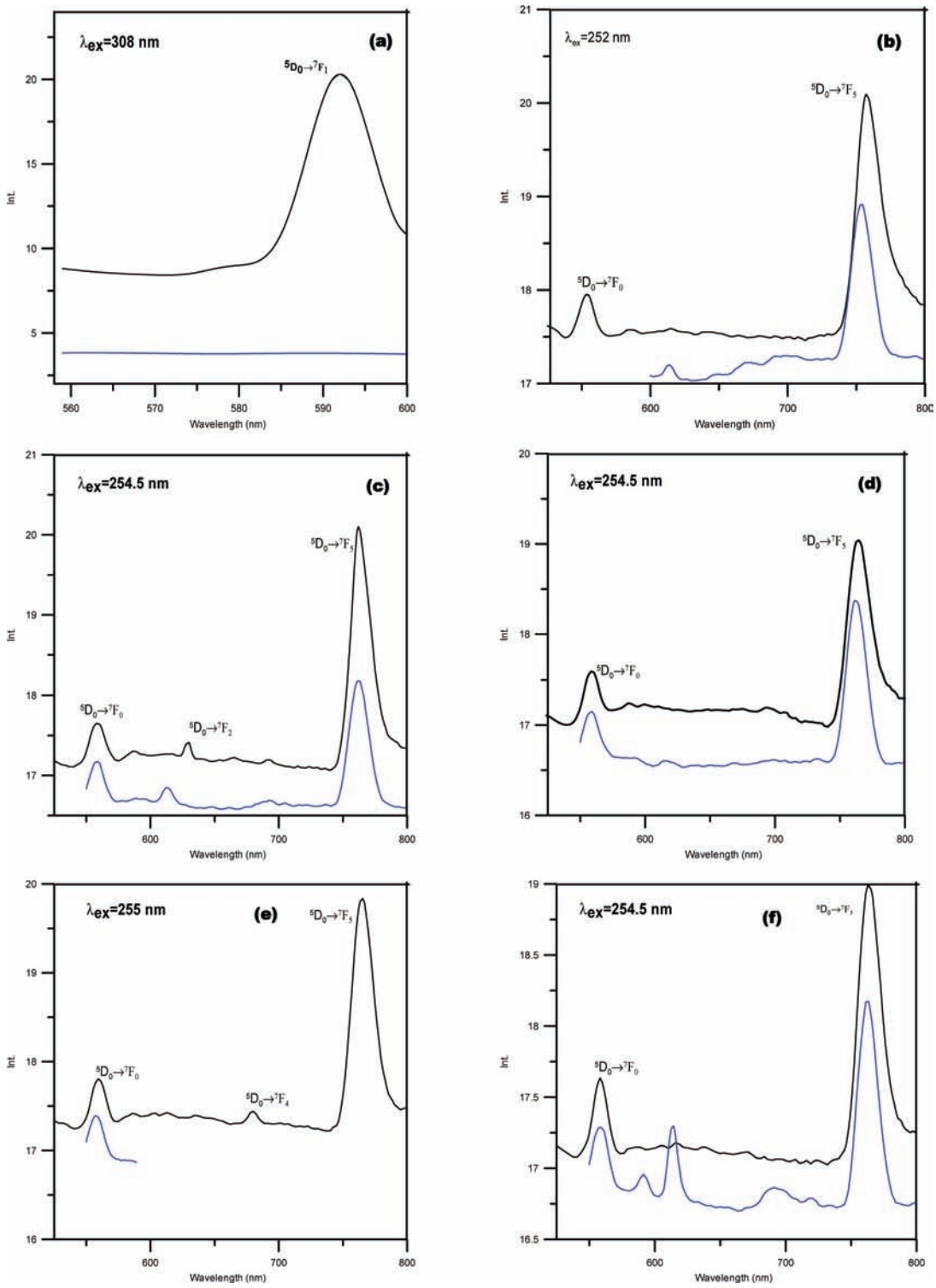


**Figure 5.** Emission spectra for $Eu^{3+}$−*N*-acetylamino acid (NAA) binary complexes at $t = (25.0 \pm 0.1)$ °C, pH = 6.5 to 7.0, $[Eu^{3+}] = [NAA] = 1 \cdot 10^{-5}$ mol·dm$^{-3}$. (a) *N*-Acetylaspartic acid. (b) *N*-Acetylhistidine. (c) *N*-Acetylglutamic acid. (d) *N*-Acetylhistamine. (e) *N*-Acetylleucine. (f) *N*-Acetyllysine. Black line, $Eu^{3+}$−*N*-acetylamino acid binary complex; blue line, *N*-acetylamino acid free ligand.

the ligand molecule to the Eu(III) metal ion. Comparing the emission spectra for the Eu(III)−*N*-acetylhistamine binary complex and the free ligand *N*-acetylhistamine indicates that the two emission bands at (559 and 762) nm could be assigned to the binary complex as $^5D_0 \rightarrow {}^7F_0$ and $^5D_0 \rightarrow {}^7F_7$ transitions with enhancement of the emission peaks. It is clearly observed that the increase in the band located at 762 nm is of a low value (0.62) for Eu(III)−*N*-acetylhistamine, hence it could be concluded that the energy transfer from *N*-acetylhistidine to Eu(III) is about 2 times that of *N*-acetylhistamine. In other words, the first one is a better sensitizer for Eu(III) than the latter. Eu(III)−*N*-acetylhistamine was only very weakly luminescent due to efficient nonradiative deactivation processes. We discovered that Eu(III)−*N*-aectylhistidine can be considered as one of the members of the novel class of lanthanide compounds that emit in the near-infrared which could open up new possibilities for the use of NIR in biological imaging as well as

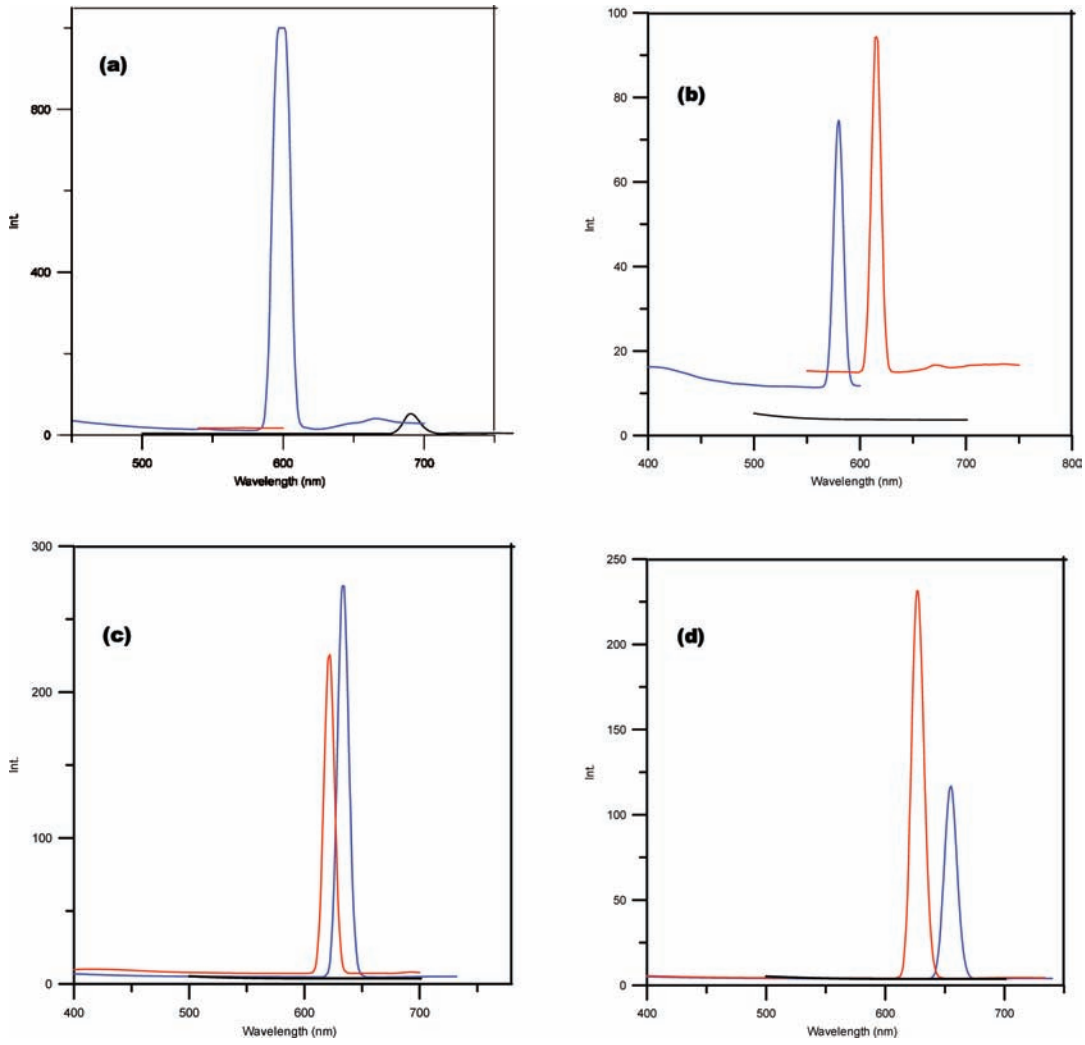


**Figure 6.** Comparative emission spectra for $Eu^{3+}$−*N*-acetylaspartic acid (NAA)−nucleotide (NU) ternary complexes at $t = (25.0 \pm 0.1)$ °C, pH = 6.5 to 7.0, $[Eu^{3+}] = [NAA] = [NU] = 1 \cdot 10^{-5}$ mol·dm$^{-3}$. (a) 5′-AMP. (b) 5′-CMP. (c) 5′-GMP. (d) 5′-ATP. Black line, $Eu^{3+}$ + *N*-acetylaspartic acid binary complex; red line, $Eu^{3+}$ + nucleotide binary complex; blue line, $Eu^{3+}$ + *N*-acetylaspartic acid + nucleotide ternary complex.

leading to materials for optical amplifiers and light-emitting diodes (LEDs) operating at telecommunication frequencies.

Comparing *N*-acetyllysine and *N*-acetylleucine emission spectra and their corresponding binary complexes with Eu(III) indicates that two peaks are observed at $\lambda$ 554 and 755 nm for the free ligands. Eu(III)-*N*-acetyllysine has the same emission bands but of higher intensity. The increase in the longer wavelength emission peak is about 1 a.$\mu$. For Eu(III)-*N*-acetylleucine three emission bands are obtained at (554, 675 and 755) nm. The emission peak which is observed at 675 nm may be assigned to a $^5D_0 \rightarrow {}^7F_4$ transition. The third peak which is located at 755 nm is enhanced upon coordination to Eu(III) by 1.4 a.$\mu$ i.e. the intramolecular energy transfer from *N*-acetylleucine to Eu(III) is higher than that in the case of *N*-acetyllysine.Figure 6.

For the Eu(III)−*N*-acetylglutamic binary complex, the emission peaks observed in the spectra for the amino acid are enhanced in intensity upon formation of the binary complex. The three emission peaks for the Eu(III)−*N*-acetylglutamic binary complex could be assigned to $^5D_0 \rightarrow {}^7F_0$, $^5D_0 \rightarrow {}^7F_2$, and $^5D_0 \rightarrow {}^7F_5$ transitions. The third peak is enhanced by about 1.8 au in intensity compared to the free ligand. Hence, *N*-acetylglutamic acid is the more effective ligand for intramolecular energy transfer to Eu(III) ions.

The binary complex Eu(III)−*N*-acetylaspartic acid has one emission peak at 595 nm which could be attributed to a $^5D_0 \rightarrow {}^7F_1$ transition. The free ligand does not exhibit any emission peak in the visible region, where energy is transferred from the lanthanide metal ion to the ligand molecule.

Comparison between the emission spectra for Eu(III)−*N*-acetylaspartic acid and the nucleotides 5′-GMP, 5′-AMP, 5′-CMP, and 5′-ATP is shown in Figure 6. Considering that Eu(III) will bind first to 5′-GMP forming the Eu(III)−5′-GMP complex, when *N*-acetylaspartic acid reacts with this binary complex forming a ternary one the emission peaks are increased by about 100 au in intensity. For the Eu(III)−5′-CMP binary complex, the interaction of *N*-acetylaspartic acid with this complex will reduce the intensity of the ternary species by about 20 au in intensity. This means that the combination of Eu(III) with the 5′-CMP molecule will decrease the probability of energy transfer from the *N*-acetylspartic acid molecule to Eu(III) in contrast to the case of complexes containing the purine nucleotide type 5′-GMP.

Since both the 5′-ATP nucleotide molecule and *N*-acetylaspartic acid can scavenge energy from the Eu(III) metal ion, the emission peak for Eu(III)−5′-ATP is lowered by about 100 au intensity when *N*-acetylaspartic acid reacts with Eu(III)−5′-ATP to form the mixed ligand complex.

Comparing the emission spectra for Eu(III)−5′-AMP, Eu(III)−*N*-acetylaspartic acid, and the corresponding ternary complex, it is clearly observed that both the binary complex species acquire very low emission bands in the visible region and that the

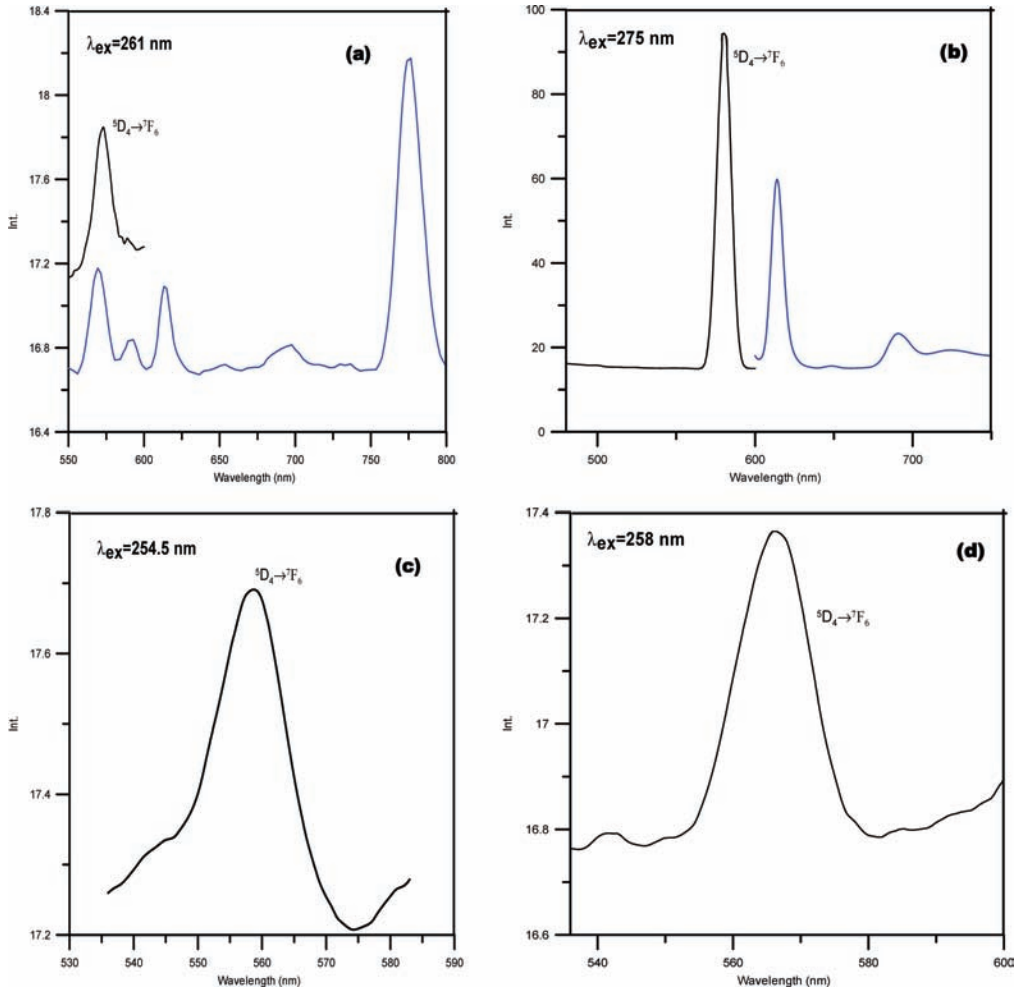


**Figure 7.** Emission spectra for $Tb^{3+}$−nucleotide (NU) binary complexes at $t = (25.0 \pm 0.1)$ °C, pH = 6.5 to 7.0, $[Tb^{3+}] = [NU] = 1 \cdot 10^{-5}$ mol·dm$^{-3}$. (a) 5′-AMP. (b) 5′-CMP. (c) 5′-GMP. (d) 5′-ATP. Black line, $Tb^{3+}$−nucleotide binary complex; blue line, nucleotide free ligand.

coordination of *N*-acetylaspartic acid with the Eu(III)−5′-AMP binary complex greatly enhances the emission spectra of the ternary complex. This behavior can be attributed to the fact that *N*-acetylaspartic acid is a good sensitizer for Eu(III) when combined with the 5′-AMP nucleotide. The assignments of emission bands for the Eu(III) complexes agree with those reported in the literature.[59−63]

***Emission Spectra for Tb(III) Complexes.*** The emission spectra of Tb(III)−nucleotide binary complexes are shown in Figure 7. The Tb(III)−5′-GMP binary complex has one emission peak at $\lambda$ 557 nm which may be attributed to a $^5D_4 \rightarrow ^7F_5$ transition. The free ligand does not give any emission peak in the range of the binary complex.

For the binary complexes containing Tb(III)−5′-AMP, only one emission peak is obtained at 572 nm which could be assigned to a $^5D_4 \rightarrow ^7F_4$ transition.The free ligand 5′-AMP has two emission bands at (557 and 572) nm, and the second peak is enhanced in its intensity upon formation of the binary complex Tb(III)−5′-AMP. The molecule of the pyrimidine nucleotide type 5′-CMP exhibits only one peak in the emission visible range of Tb(III)−5′-CMP at 490 nm of about 18.00 au intensity. The binary complex acquires one peak at $\lambda$ 580 nm which could be assigned to a $^5D_4 \rightarrow ^7F_4$ transition of high intensity (≈93.00 au). This means that there is a great probability of energy transfer from the free metal ion Tb(III) to the nucleotide molecule.

The Tb(III)−5′-ATP binary complex has one emission peak which takes place at $\lambda = 575$ nm which could be assigned to a ($^5D_4 \rightarrow ^7F_4$) transition, and the free ligand has no emission peak within the visible range of emission for Tb(III)−5′-ATP; i.e., there is energy transfer from the Tb(III)-f-electrons to the nucleotide molecule.

The binary complex Tb(III)−*N*-acetylhistidine acquires two emission peaks at (544 and 563) nm, and such peaks are the characteristics ones for $^5D_4 \rightarrow ^7F_5$ and $^5D_4 \rightarrow ^7F_4$ transitions.

The free ligand has no emission peaks within the visible range for Tb(III) complexes as shown in Figure 8.

In contrast, Tb(III)−*N*-acetylhistamine has three emission peaks at (544, 562, and 586) nm. The *N*-acetylhistamine has one emission peak at $\lambda$ 550 nm. The most interesting feature is that *N*-acetylhistamine has the probability to donate energy to Tb(III) where different types of transitions occur, while the analogue imidazole containing amino acid *N*-acetylhistidine does not exhibit this probability for energy donation [Figure 8(d, b)].

Comparing Tb(III)−*N*-acetylleucine and Tb(III)−*N*-acetyllysine binary complexes, with the emission spectra for the two ligands, the binary complexes have three types of transition at (544, 556, and 585) nm, and the two amino acids have a similar probability of energy transfer to the Tb(III) as shown in [Figure 8(e, f)].

The *N*-acetylglutamic molecule has one emission peak at $\lambda$ 560 nm, where the corresponding binary complex Tb(III)−*N*-acetylglutamic acid exhibits three emission peaks, where energy is transferred from the *N*-acetylamino acid to Tb(III). The corresponding dicarboxylic acid *N*-acetylaspartic acid

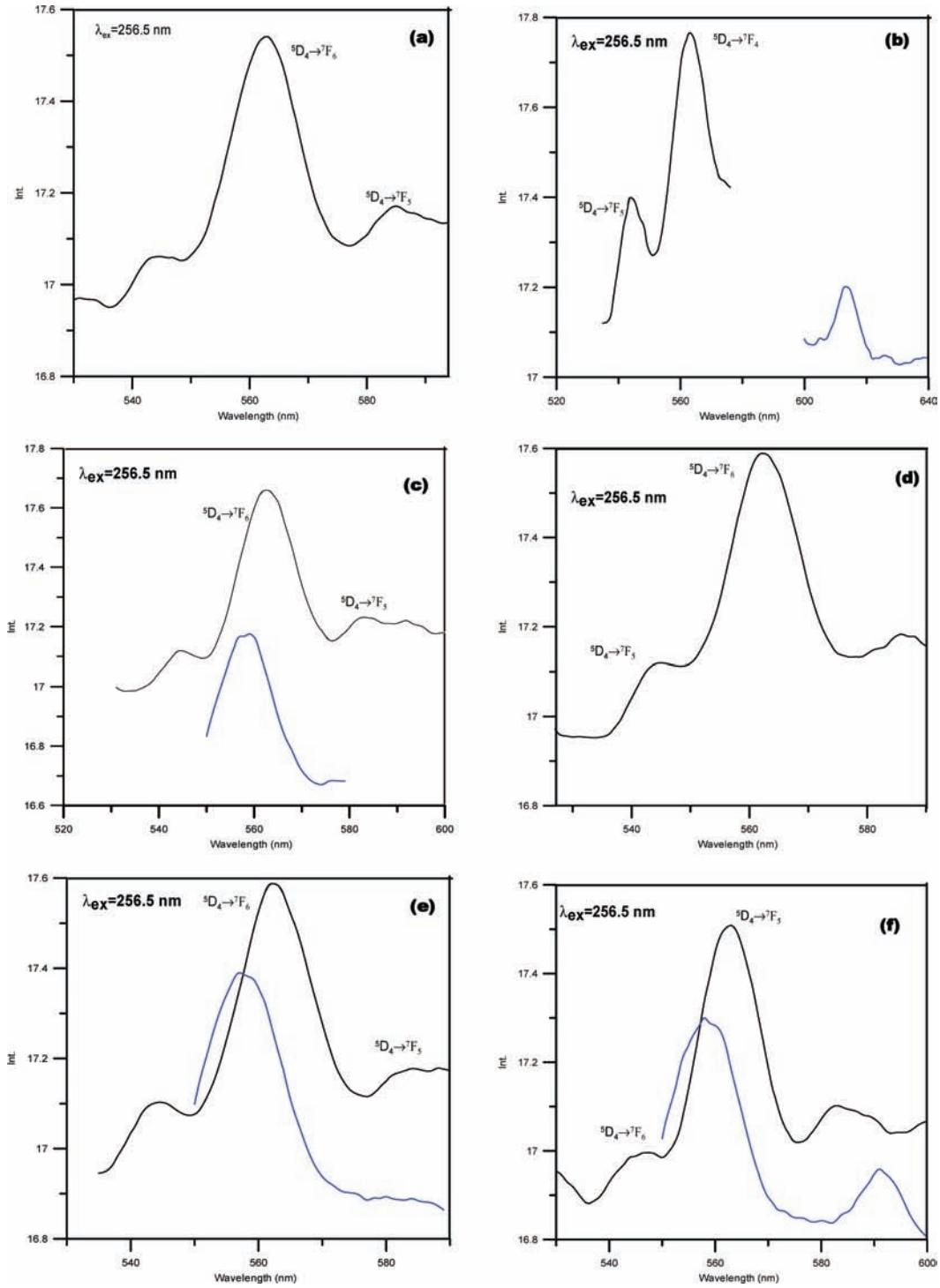


**Figure 8.** Emission spectra for $Tb^{3+}$−*N*-acetylamino acid (NAA) binary complexes at $t = (25.0 \pm 0.1)$ °C, pH = 6.5 to 7.0, $[Tb^{3+}] = [NAA] = 1 \cdot 10^{-5}$ mol·dm$^{-3}$. (a) *N*-Acetylaspartic acid. (b) *N*-Acetylhistidine. (c) *N*-Acetylglutamic acid. (d) *N*-Acetylhistamine. (e) *N*-Acetylleucine. (f) *N*-Acetyllysine. Black line, $Tb^{3+}$−*N*-acetylamino acid binary complex; blue line, *N*-acetylamino acid free ligand.

does not exhibit any emission peak within the range of visible emission for Tb(III). There is a considerable probability of energy transfer from the Tb(III) to the *N*-acetylamino acid as shown in Figure 8.

The quenching effect of *N*-acetylaspartic acid on the emission spectra for Tb(III)−AMP has been observed (figure is not shown in the text) where the emission intensity of the mixed ligand complex Tb(III)−5′-AMP−*N*-acetylaspartic acid is lower than that of Tb(III)−5′-AMP by 25 au in intensity.

A contrasting behavior is observed for the ternary complex Tb(III)−5′-CMP−*N*-acetylaspartic acid where the reaction of the amino acid with Tb(III)−5′-CMP will enhance the emission intensity by 40 au where the amino acid residue cannot act as a scavenger of energy from Tb(III) when it is binded to the 5′-CMP molecule.

Emission spectra for Tb(III)−5′-GMP and Tb(III)−*N*-acetylaspartic acid with the ternary complex containing the two ligands have been investigated. The emission spectra of the mixed ligand complex are completely different from those of the two binary ones. It has an emission peak at $\lambda = 490$ nm which is characteristic for a $^5D_4 \rightarrow {}^7F_6$ transition.

The 5′-AMP molecule will donate energy to Tb(III), but the *N*-acetylaspartic acid has an ability to scavenge energy from the lanthanide metal ion. Hence the synergistic effect is the increase in emission for the ternary complex species.

The most important interesting feature is the enhanced fluorescence observed during the interaction of *N*-acetylaspartic with the Tb(III)−5′-ATP binary complex, and the ternary complex species acquires a more intense peak than the two binary ones where the combination of Tb(III) to the nucleotide molecule (5′-ATP) will promote the ability of *N*-acetylaspartic acid to donate energy. The assignments of emission bands for the Tb(III) complexes may be according to the results in the literature.[59,63,64]

## Conclusions

In the present study, potentiometric equilibrium measurements have been performed at (25.0 ± 0.1) °C and ionic strength $I$ = 0.1 mol·dm$^{-3}$ $KNO_3$ for the interaction of biologically important ligands *N*-acetyl histidine, *N*-acetyl L-leucine, *N*-acetylglutamic acid, *N*-acetylhistamine, *N*-acetylaspartic acid, and La(III), Gd(III), Sm(III), Tb(III), Eu(III), and Dy(III) with the nucleotides guanosine 5′-monophosphate (5′-GMP), cytedine 5′-monophosphate (5′-CMP), inosine 5′-monophosphate (5′-IMP), adenosine 5′-monophosphate (5′-AMP), adenosine 5′-diphosphate (5′-ADP), adenosine 5′-triphosphate (5′-ATP), and cytedine 5′-triphosphate (5′-CTP) in 1:1:1 and 1:2:1 ratios. The results confirm the possible recognition of the purine and pyrimidine mononucleotides by *N*-acetyl amino acid complexes of lanthanides in aqueous media. This important biochemical process has been confirmed by UV spectroscopic and fluorimetric measurements. Therefore, the studied ternary systems can be considered as models for development of chemo- and biosensors incorporating moleculary imprinted polymers for selective detection of the nucleotide under investigation. Moleculary imprinted polymers containing Eu(III) and Tb(III) will be of special interest in developing luminescent-based chemo- and biosensors for the detection of *N*-acetyl amino acids included in this study.

## Literature Cited


(1) Steinkamp, T.; Karst, U. Detection strategies for bioassays based on luminescent lanthanide complexes and signal amplification. *Anal. Bioanal. Chem.* **2004**, 24–30.

(2) Baslow, M. H. A review of phylogenetic and metabolic relationships between the acylamino acids, N-acetyl-l-aspartic acid & N-acetyl-l-histidine in the vertebrate nervous system. *J. Neurochem.* **1979**, *68* (4), 1335–1334.

(3) Baslow, M. H. Evidence supporting a role for N-acetyl-l-aspartate as a molecular water pump in myelinated neurons in the central nervous system an analytical review. *Neurochem. Int.* **2002**, *40* (4), 295–300.

(4) Hummer, G.; Garcia, A. E.; Soumpasis, D. M. A statistical mechanical description of biomolecular hydration. *Faraday Discuss.* **1996**, *103*, 175–189.

(5) Baslow, M. H. The existence of molecular water pumps in the nervous system. A review of evidence. *Neurochem. Int.* **1999**, *34*, 77–90.

(6) Applewhite, T. H.; Niemann, C. The Interaction of α-Chymotrypsin with a Series of α-N-Acetyl-α-amino Acid Methylamides. *J. Am. Chem. Soc.* **1958**, *81*, 2208–2213.

(7) Tallan, H. H.; Moore, S.; Stein, W. H. N-Acetyl-l-aspartic acid in brain. *J. Biol. Chem.* **1956**, *219*, 257–264.

(8) Birken, D. L.; Oldendorf, W. H. N-acetyl-L-aspartic acid: a literature review of a compound prominent in 1H-NMR spectroscopic studies of brain. *Neurosci. Biobehav. Rev.* **1989**, *13*, 23–31.

(9) Tsai, G.; Coyle, J. T. N-Acetylaspartate in neuropsychiatric disorders. *Prog. Neurobiol.* **1995**, *46*, 531–540.

(10) Goldstein, F. B. Biosynthesis of N-acetyl-l-aspartic acid. *J. Biol. Chem.* **1959**, *234*, 2702–2706.

(11) Knizley, H., Jr. The enzymatic synthesis of N-acetyl-l-aspartic acid by a water insoluble preparation of a cat brain acetone powder. *J. Biol. Chem.* **1967**, *242*, 4619–4622.

(12) Truckenmiller, M. E.; Namboodiri, M. A. A.; Brownstein, M. J.; Neale, J. H. N-Acetylation of l-aspartate in the nervous system: differential distribution of a specific enzyme. *J. Neurochem.* **1985**, *45*, 1658–1662.

(13) Moffett, J. R.; Namboodiri, M. A. A.; Cangro, C.; Neale, J. H. Immunochemical localization of N-acetylaspartate in rat brain. *Neuroreport* **1991**, *2*, 131–134.

(14) Simmons, M. L.; Frondoza, C. G.; Coyle, J. T. Immunocytochemical localization of N-acetylaspartate with monoclonal antibodies. *Neuroscience* **1991**, *45*, 37–45.

(15) Moffett, J. R.; Namboodiri, M. A. A. Differential distribution of N-acetylaspartylglutamate and N-acetylaspartate immunoreactivities in the rat brain. *J. Neurocytol.* **1995**, *24*, 409–433.

(16) Bhakoo, K. K.; Pearce, D. In vitro expression of N-acetylaspartate by oligodendrocytes: implications for proton magnetic resonance spectroscopy signal in vivo. *J. Neurochem.* **2000**, *74*, 254–262.

(17) Jung, R. E.; Yeo, R. A.; Chiulli, S. J.; Sibbitt, W. L.; Weers, D. C.; Hart, B. L.; Brooks, W. M. Biochemical markers of cognition: a proton MR spectroscopy study of normal human brain. *Neuroreport* **1999**, *10*, 3327–3331.

(18) Jung, R. E.; Brooks, W. M.; Yeo, R. A.; Chiulli, S. J.; Weers, D. C.; Sibbitt, W. L. Biochemical markers of intelligence: a proton MR spectroscopy study of normal human brain. *Proc. R. Soc. London B* **1999b**, *266*, 1375–1379.

(19) Matalon, R.; Michals, K.; Kaul, R. Canavan disease: from spongy degeneration to molecular analysis. *J. Pediatr.* **1995**, *127*, 511–517.

(20) Patel, T. B.; Clark, J. B. Synthesis of N-acetyl-L-aspartate by rat brain mitochondria and its involvement in mito-chondrial/cytosolic carbon transport. *J. Biochem.* **1979**, *184*, 539–546.

(21) Bates, T. E.; Strangward, M.; Keelan, J.; Davey, G. P.; Munro, P. M.; Clark, J. B. Inhibition of N-acetylaspartate production: Implications for ′H MRS studies in vivo. *Neuroreport* **1996**, *7*, 1397–1400.

(22) Baslow, M. H. A review of phylogenetic and metabolic relation ships between the acylamino acids, N-acetyl-L L-aspartic acid and N-acetyl-L L-histidine, in the vertebrate nervous system. *J. Neurochem.* **1997**, *68*, 1335–1344.

(23) Clark, J. B. N-Acetyl aspartate: a marker for neuronal loss or mitochondrial dysfunction. *Dev. Neurosci.* **1998**, *20*, 271–276.

(24) Tsai, G.; Coyle, J. T. N-Acetylaspartate in neuropsychiatric disorders. *Prog. Neurobiol.* **1995**, *46*, 531–540.

(25) Jacobs, M. A.; Horska, A.; van Zijl, P. C.; Barker, P. B. Quantitative proton MR spectroscopic imaging of normal human cerebellum and brain stem. *Magn. Reson. Med.* **2001**, *46*, 699–705.

(26) Wang, Y.; Li, S. J. Differentiation of metabolic concentrations between gray matter and white matter of human brain by in vivo H magnetic resonance spectroscopy. *Magn. Reson. Med.* **1988**, *39*, 28–33.

(27) Pouwels, P. J.; Frahm, J. Differential distribution of NAA and NAAG in human brain as determined by quantitative localized proton MRS. *NMR Biomed.* **1997**, *10*, 73–78.

(28) Soher, B. J.; van Zijl, P. C.; Duyn, J. H.; Barker, P. B. Quantitative proton MR spectroscopic imaging of the human brain. *Magn. Reson. Med.* **1996**, *35*, 356–363.

(29) Friedman, S. D.; Brooks, W. M.; Jung, R. E.; Hart, B. L.; Yeo, R. A. Proton MR spectroscopic findings correspond to neuropsychological function in traumatic brain injury. *AJNR Am. J. Neuroradiol.* **1998**, *19*, 1879–1885.

(30) Baslow, M. H. N-Acetylaspartate in the vertebrate brain: metabolism and function. *Neurochem. Res.* **2003**, *28*, 941–953.

(31) Jenkins, B. G.; Klivenyi, P.; Kustermann, E.; Andreassen, O. A.; Ferrante, R. J.; Rosen, B. R.; Beal, M. F. Nonlinear decrease over time in N-acetyl aspartate levels in the absence of neuronal loss and increases in glutamine and glucose transgenic Huntington's disease mice. *J. Neurochem.* **2000**, *74*, 2108–2119.

(32) Suhy, J.; Miller, R. G.; Rule, R.; Schu, N.; Licht, J.; Dronsky, V.; Gelinas, D.; Maudsley, A. A.; Weiner, M. W. Early detection and longitudinal changes in amyotrophic lateral sclerosis by (1)H MRSI. *Neurology* **2002**, *58*, 773–779.

(33) Huang, W.; Alexander, G. E.; Chang, L.; Shetty, H. U.; Krasuski, J. S.; Rapoport, S. I.; Schapiro, M. B. Brain metabolite concentration and dementia severity in Alzheimer's disease: a (1)H MRS study. *Neurology* **2001**, *57*, 626–632.

(34) Konaka, K.; Ueda, H.; Li, J. Y.; Matsumoto, M.; Sakoda, S.; Yanagihara, T. N-Acetylaspartate to total creatine ratio in the hippocampal CA1 sector after transient cerebral ischemia in gerbils: influence of neuronal elements, reactive gliosis, and tissue atrophy. *J. Cereb. Blood Flow Metab.* **2003**, *23*, 700–708.

(35) Wylezinska, M.; Cifelli, A.; Jezzard, P.; Palace, J.; Alecci, M.; Matthews, P. M. halamic neurodegeneration in relapsing-remitting multiple sclerosis. *Neurology* **2003**, *60*, 1949–1954.

(36) Iranzo, A.; Moreno, A.; Pujol, J.; Marti-Fabregas, J.; Domingo, P.; Molet, J.; Ris, J.; Cadafalch, J. Proton magnetic resonance spectroscopy pattern progressive multifocal leukoencephalopathy in AIDS. *J. Neurol. Neurosurg. Psychiatry* **1999**, *66*, 520–523.

(37) Yamasue, H.; Fukui, T.; Fukuda, R.; Yamada, H.; Yamasaki, S.; Kuroki, N.; Abe, O.; Kasai, K.; Tsujii, K.; Iwanami, A.; Aoki, S.; Ohtomo, K.; Kato, N.; Kato, T. (1)H-MR spectroscopy and gray matter volume of the anterior cingulate cortex in schizophrenia. *Neuroreport* **2002**, *13*, 2133–2137.
(38) Baslow, M. H. The existence of molecular water pumps in the nervous system. A review of the evidence. *Neurochem. Int.* **1999b**, *34*, 77–90.
(39) Urenjak J.; Obrenovitch T. P.; Richards D.; Williams S. R.; Symon L. Is N-acetyl-aspartate involved in neurotransmission: A microdialysis study. In *Monitoring Molecules in Neuroscience*; University Center for Pharmacy: Groningen, 1991; pp 355−357.
(40) Wroblewska, B.; Santi, M. R.; Neale, J. H. N-Acetylaspartylglutamate activates cyclic AMP-coupled metabotropic glutamate receptors in cerebellar astrocytes. *Glia* **1998**, *24*, 172–179.
(41) Schoepp, D. D.; Jane, D. E.; Monn, J. A. Pharmacological agents acting at subtypes of metabotropic glutamate receptors. *Neuropharmacology* **1999**, *38*, 1431–1476.
(42) Anwar, Z. M.; Azab, H. A. Ternary complexes formed by trivalent lanthanide ions, nucleotides, and biological buffers. *J. Chem. Eng. Data* **2001**, *46*, 613–618.
(43) ESAB2M: De Stefano, C.; Princi, P.; Ringo, C.; Sammartano, S. Computer analysis of equilibrium data in solution ESAB2M: An improved version of the ESAB program. *Ann. Chim. (Rome)* **1987**, *77*, 643–675.
(44) Gans, P.; Sabatini, A.; Vacca, A. SUPERQUAD: An improved general program for computatiom of formation constants from potentiometric data. *J. Chem. Soc., Dalton Trans.* **1985**, 1195–1200.
(45) Martell, A. E.; Sillen, L. G. *Stability Constants of Metal Ion Complexes*; The Chemical Society: London, 1971.
(46) Ringbom, A. *Complexation in Analytical Chemistry*; Wiley-Inter-Sciences: New York, 1963.
(47) Perrin, D. D.; Dempsey, B. *Buffers for pH and Metal Ion Control*; Chapman and Hall: London, 1979.
(48) NIST Standard Reference Database 46 Version 6.0 NIST Critically Selected Stability Constants of Metal Complexes.
(49) Kiss, A.; et al. Solution Equilibria of the Ternary Complexes of $[Pd(dien)Cl]^+$ and $[Pd(terpy)Cl]^+$ with Nucleobases and N-acetyl Amion Acids. *J. Inorg. Biochem.* **1997**, 85–92.
(50) Schwarzenbach, G. *Complexometric Titrations*; Interscience: New York, 1957.
(51) SC Database; Royal Society of Chemistry; IUPAC: 2004; http://www.Acadsoft.Co.uK/.
(52) Cornelis, R.; Caruso, J.; Crews,H.; Heumann, K. *Handbook of Elemental speciation: Techniques and Methodology*; Wiley: New York, 2003.
(53) Jurek, E. R. P.; Jurk, M. A.; Martell, E. A. Phosphate diester hydrolysis by mono-and dinuclear lanthanum complexes with an unusual third-order dependence. *Inorg. Chem.* **2000**, *39*, 1016–1020.
(54) Bazilevskaya, N. S.; Cherkasov, A. S. Two fluorescence bands of meso- anthracene carboxylic acid and of the excimer. *Zh. Prikl. Spektrosk.* **1965**, *3* (6), 548–55.
(55) Bazilevskaya, N. S.; Cherkasov, A. S. Excitation of the dimmers of derivatives of anthracene.1-Acetoxy anthracene and anthracene-9-carboxylic acids. *Opt. Spektrosk.* **1965**, *18*, 58–62, No.1.
(56) Werner, T. C.; Hercules, D. M. The fluorescence of 9-anthroic acid and its esters. Environmental effects on excited-state behaviour. *J. Phys. Chem.* **1969**, *73* (6), 2005–2011.
(57) Werner, T. C.; Hercules, D. M. Charge-transfer effects on the absorption and fluorescence spectra of anthroic acids. *J. Phys. Chem.* **1970**, *74* (5), 1030–1037.
(58) Cown, D. O.; Schmiegel, W. W. Photodimerization of 9-anthroic acid and sodium 9-anthroate. *J. Am. Chem. Soc.* **1972**, *94* (19), 6779–6788.
(59) Ping, L.; Dong, L.; Zhen, T.; Xinxing, L. Synthesis and Luminescence propereties of novel Europium and Terbium complexes with triblock copolymer ligand. *Macromolecules* **2002**, *35*, 1487–1488.
(60) Christopher, G. G.; Theresa, M. R. Synthesis, Characterization, and Luminescence propereties of a new series of $Eu^{3+}$containing Macrocycles. *Inorg. Chem.* **2005**, *44*, 9829–9836.
(61) Deping, G.; Zuqiang, B.; Kezhi, W.; Linnpei, J.; Chun-Hui, H. Synthesis and electroluminescence propereties of an organic europium complex. *J. Alloys Compd.* **2003**, *358*, 188–192.
(62) Frantini, A.; Swavey, S. Luminescent and structural properties of $Eu^{3+}$ complex: Formation of a one dimensional array bridged by 2,2′-bibyrimidine. *Inorg. Chem. Commun.* **2007**, *10*, 636–638.
(63) Bing, X.; Bing, Y. Photophysical properties of novel Lanthanide ($Tb^{3+}$, $Dy^{3+}$, $Eu^{3+}$) complexes with long chain para-carboxyphenol ester P-L-benzoate (*L*= dodecanoyloxy, myristoyloxy, palmitoyloxy and stearoyloxy. *Spectra Chim. Acta* **2007**, 236–242, part A66.
(64) Fangfang, D.; Weisheng, L. Enhanced Fluorescence of 3-tryptimino-1-phenyl-butan-1-one-$Tb^{3+}$ with 1,10-phenanthroline ternary system, and its analytical application. *Michrochim. Acta* **2007**, *158*, 111–116.

Received for review May 9, 2009. Accepted September 6, 2009.

JE9004118